# Building and Destroying Continental Mantle

Cin-Ty A. Lee, Peter Luffi, and Emily J. Chin

Department of Earth Sciences, Rice University, Houston, Texas 77005; email: ctlee@rice.edu

Annu. Rev. Earth Planet. Sci. 2011. 39:59–90

First published online as a Review in Advance on January 5, 2011

The *Annual Review of Earth and Planetary Sciences* is online at earth.annualreviews.org

This article's doi:
10.1146/annurev-earth-040610-133505



0084-6597/11/0530-0059$20.00

## Keywords

craton, peridotite, eclogite, tectosphere, boundary layer, geochemistry

## Abstract

Continents, especially their Archean cores, are underlain by thick thermal boundary layers that have been largely isolated from the convecting mantle over billion-year timescales, far exceeding the life span of oceanic thermal boundary layers. This longevity is promoted by the fact that continents are underlain by highly melt-depleted peridotites, which result in a chemically distinct boundary layer that is intrinsically buoyant and strong (owing to dehydration). This chemical boundary layer counteracts the destabilizing effect of the cold thermal state of continents. The compositions of cratonic peridotites require formation at shallower depths than they currently reside, suggesting that the building blocks of continents formed in oceanic or arc environments and became "continental" after significant thickening or underthrusting. Continents are difficult to destroy, but refertilization and rehydration of continental mantle by the passage of melts can nullify the unique stabilizing composition of continents.

## INTRODUCTION

Ocean basins are the surface expression of solid-state mantle convection with a mobile lid. Heat transfer in Earth's deep interior is driven by thermally buoyant upwellings, but when the upwelling reaches the surface of Earth, the mechanism of vertical heat transfer becomes dominated by conduction, and a cold upper thermal boundary layer is generated. Progressive cooling makes this thermal boundary layer thicken and contract, causing it to eventually downwell in the form of a subducting slab. Continents, however, are underlain by much thicker and hence cooler thermal boundary layers, but unlike ocean basins, they have survived for billions of years, far longer than the <200-Ma life span of ocean basins. This apparent paradox can be resolved if the negative thermal buoyancies of continents are compensated by intrinsic chemical buoyancy. Motivated by the lack of free-air gravity anomalies over continents (implying that continents are in isostatic equilibrium), Jordan proposed the isopycnic (iso = equal, pycnic = density) hypothesis: Continental mantle is made up of low-density, melt-depleted peridotite residua, whose low densities exactly offset the effect of thermal contraction associated with a growing thermal boundary layer (Jordan 1978, 1988). In Jordan's view, this chemical boundary layer would equate with the thermal boundary layer; he referred to this concept as the tectosphere.

To first order, Jordan's hypothesis has proven correct, but important questions remain. Net neutral buoyancy or isostatic equilibrium alone may not ensure stability. Specifically, if at any moment perfectly isopycnic conditions are not met, lateral pressure gradients will drive (upward) gravitational collapse of continental thermal boundary layers. The longevity of continental mantle demands an intrinsically stronger (more viscous) mantle, which effectively renders continents as rigid boundary layers physically isolated from the convecting mantle (Cooper et al. 2004, Hirth & Kohlstedt 1996, Lee et al. 2005, Lenardic et al. 2003). One widely accepted hypothesis is that continental mantle is composed of melt-depleted and dehydrated peridotites, making such mantle considerably more viscous than the "wetter," convecting mantle (Hirth & Kohlstedt 1996, Pollack 1986). As we discuss below, this melt-depleted chemical boundary layer would coincidentally correspond to a rheological boundary layer.

Because the composition of continental mantle appears to play such an important role in its dynamic evolution, understanding how such mantle forms is important. Excellent reviews on the nature and origin of continental mantle, each from the perspective of a different field (e.g., petrology/geochemistry, geodynamics, and geophysics), already exist (Arndt et al. 2009, Canil 2008, Eaton et al. 2009, Griffin et al. 2003, King 2005, Lee 2006, Lee et al. 2005, Lenardic et al. 2003, Pearson et al. 2003, Pearson & Wittig 2008, Simon et al. 2007, Sleep 2004). We build on this foundation by providing a perspective that integrates petrology, geochemistry, and geophysics to improve our understanding of the petrogenetic and tectonic processes involved in forming continental mantle. By establishing the necessary conditions for stabilizing continental mantle, we also discuss what processes may be responsible for its chemical modification and destruction.

## TERMINOLOGY

A few definitions are in order. Lithosphere denotes the mechanically strong layer that effectively acts like a rigid plate. The term is often improperly used to describe a geochemically enriched layer or the seismic lid. To avoid confusion, we use the generic term boundary layer to describe the region of the uppermost mantle where a particular physical or chemical property changes. The upper thermal boundary layer (as opposed to the lower thermal boundary layer, which would be located at the core-mantle boundary) is the uppermost part of Earth, wherein the thermal state is approximated by conductive cooling rather than by an adiabatic gradient. Its thickness

is defined by the limit at which the cooler temperatures of the boundary layer can be resolved from the mantle adiabat (which is pinned to the potential temperature of the mantle, i.e., the temperature of the convecting mantle if it were adiabatically decompressed to the surface of Earth in the solid state). Mantle viscosity increases exponentially with decreasing temperature; hence a rheological boundary layer always exists *within* a thermal boundary layer. Here, we equate this viscously defined rheological boundary layer with the lithosphere (the viscous boundary layer is thicker than the effective elastic thickness). The region of low viscosity below the lithosphere is the asthenosphere (for additional discussion, see Eaton et al. 2009). Any chemically distinct layer in the uppermost mantle is referred to as a chemical boundary layer, which includes the crust and the part of the continental mantle that is compositionally distinct (for example, melt-depleted) from the convecting mantle. The term continental mantle is used when no particular type of boundary layer is specified. In general, the thermal, rheological, and chemical boundary layers need not coincide, but under continents, all these boundary layers may coincide.



## AGE DISTRIBUTION OF CONTINENTS

The interiors of continents are cored by cratons (*kratos* is Greek for strength), regions of crustal basement that have not been deformed for >~1 Ga. Thus, cratons include Archean and Proterozoic basements (see Goodwin 1991 and Hoffman 1989). **Figure 1** shows the distribution of Precambrian (>540 Ma) cratons, including platforms overlain by sediments. Cratons can be further subdivided by age: Archean (>2.5 Ga) cratons are known as Archons, and Proterozoic cratons are known as Protons (Griffin et al. 2003). Surrounding Archons and Protons are Phanerozoic accreted terranes and orogenic belts, often referred to as tectons. Unlike cratons, the latter have been subjected to Phanerozoic tectonic deformation. Notably, not all Precambrian basements are immune to tectonic deformation. For example, early to mid-Proterozoic lithosphere in the southwestern United States has been influenced by Cenozoic Basin and Range extension (Lee et al. 2001), and the Archean North China and Wyoming cratons appear to have been recently thinned (Gao et al. 2002, Griffin et al. 1998, Menzies et al. 1993, Menzies et al. 2007).

The age distribution (**Figure 2**) of the crust is multimodal, which suggests episodicity in continent formation or destruction. Histograms of U-Pb zircon ages show peaks at 3, 2.7, 2.1, 1.7–1.8, and 1.1 Ga (Condie et al. 2009, Hawkesworth & Kemp 2006). Most of these zircon U-Pb age peaks correspond to Lu-Hf and Sm-Nd depleted-mantle model ages, so to first order, these age peaks reflect juvenile crust production (Bennett et al. 1993, Condie et al. 2009, Hawkesworth & Kemp 2006). Determining the formation age of the underlying continental mantle is more challenging because mantle xenoliths, before entrainment in the host magma, typically reside at temperatures above the closure temperature of most radiometric systems; hence their internal isochron ages often reflect eruption ages. Isotopic memory of older events is more likely preserved in whole rocks or mineral inclusions in diamonds. For example, radiogenic and unradiogenic whole-rock Sr and Nd isotopes, respectively, indicate Ga isolation in an incompatible-element-enriched environment (Cohen et al. 1984, Roden & Murthy 1985). Similarly, Nd model ages of garnet grains isolated in diamonds give Archean ages (Richardson et al. 1984). However, because Sr and Nd isotopes are incompatible elements, model ages based on these isotopic systems usually date only metasomatic events.

Better constraints on the timing of melt extraction and initial isolation from the convecting mantle are obtained from the Re-Os isotopic system (Chesley et al. 1999; Handler et al. 1997; Pearson et al. 1995a,b; Reisberg & Lorand 1995; Shirey & Walker 1998; Walker et al. 1989). In this isotopic system, the parent isotope $^{187}$Re is incompatible in the solid during melting, but the daughter isotope $^{187}$Os is compatible. Therefore, with extreme melt depletion, the residue

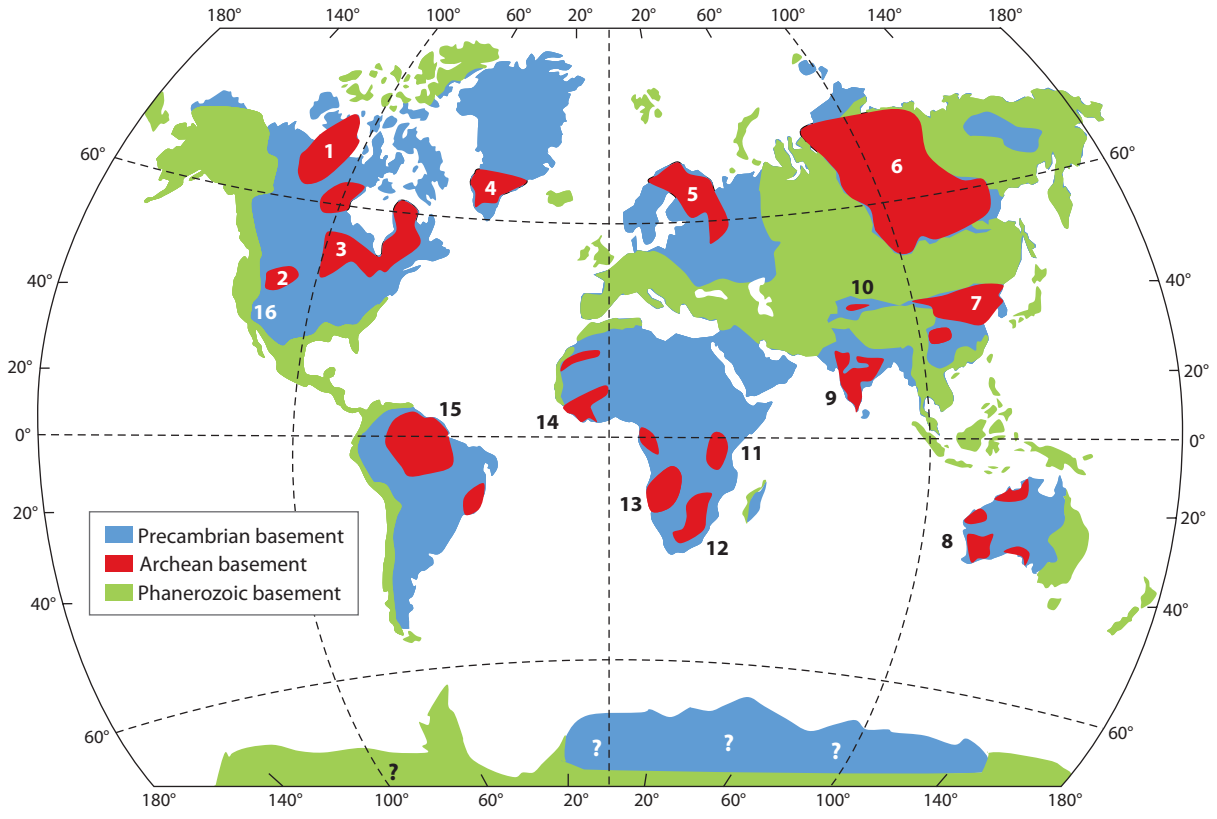


**Figure 1**

Map of Precambrian (>540 Mya) and Phanerozoic (<540 Mya) crustal basement. Archean cratons are shown in red. Cratons are labeled as follows: 1, Slave; 2, Wyoming; 3, Superior; 4, Greenland; 5, Fennoscandian; 6, Siberian; 7, North China; 8, west Australian; 9, Indian; 10, Tarim; 11, Tanzanian; 12, South African (Kaapvaal); 13, Congo; 14, west African; 15, Amazonia; 16, Colorado Plateau. Modified from Goodwin (1991) and Pearson & Wittig (2008).



"freezes" in the original $^{187}Os/^{188}Os$ of the rock, which can be used to calculate a model age for separation from the convecting mantle. The compatibility of Os also ensures that most metasomatizing agents (melts or fluids) are highly depleted in Os; hence disturbance by metasomatism is minimal. Although some complications arise from Re and platinum-group-element metasomatism (Alard et al. 2000), broad conclusions based on Re-Os model ages can be made. Whole-rock Re-Os model ages give peaks at 2.7 ± 0.3 Ga and between 1.0 and 2.0 Ga (see Carlson et al. 2005). More recently, Os isotopic measurements have been made on sulfides in peridotites and in diamond inclusions, yielding similar results (Alard et al. 2002, Pearson & Wittig 2008, Shirey et al. 2002). In summary, both continental crust and mantle formation appear to be episodic and coeval to within error (**Figure 2**).

## THICKNESS OF CONTINENTS

### Constraints from Surface Heat Flux

One of the first constraints on the thickness of continents came from surface heat flux measurements, which were used to extrapolate surface temperatures to depth assuming a

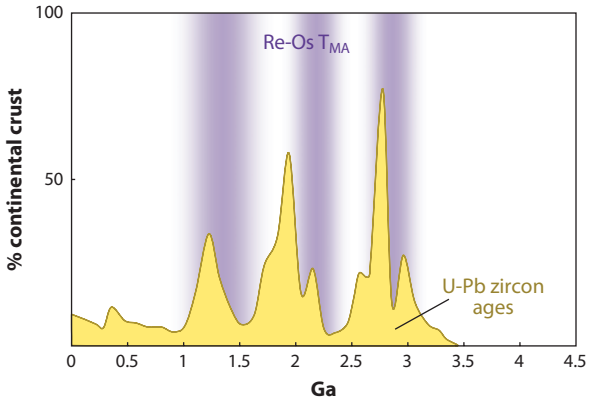


**Figure 2**

Age histogram for the crust and mantle, the former based on U-Pb radiometric dates on zircons and the latter based on Re-Os model ages. U-Pb histogram modified from Hawkesworth & Kemp (2006). Shaded areas refer to clusters of Re-Os model ages (Carlson et al. 2005). $T_{MA}$, model age.

steady-state conductive geotherm (Pollack et al. 1993). The intersection of this conductive geotherm with the mantle adiabat is equated with the base of the thermal boundary layer (**Figure 3**). Surface heat flux is generally low (30–40 mW $m^{-2}$) in Archean cratons, high (>60–80 mW $m^{-2}$) in most Phanerozoic regions, and low to intermediate in Proterozoic regions (Nyblade 1999, Pollack et al. 1993). Although some of this variation could arise from variations in

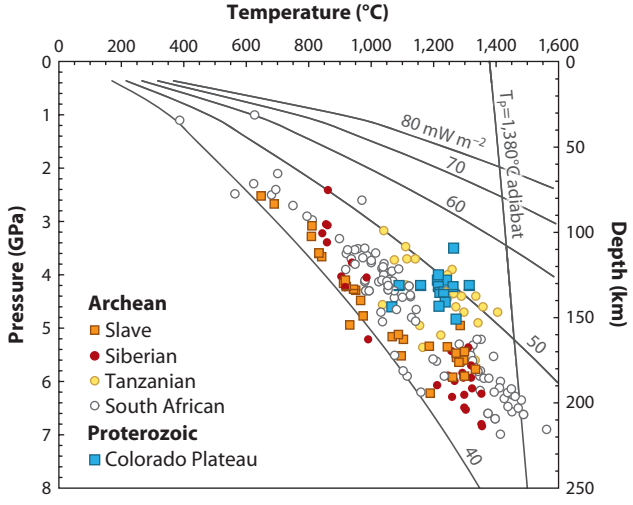


**Figure 3**

Xenolith geotherms derived from Archean and Proterozoic cratonic peridotites. Thermobarometric data are based on two-pyroxene thermometry and Al-in-orthopyroxene coexisting with garnet barometry (Brey & Kohler 1990). Mineral data for the calculations are taken from the literature (Boyd et al. 1993, Boyd et al. 1997, Carswell et al. 1979, Ehrenberg 1982, Kopylova & Russell 2000, Kopylova et al. 1999, Lee & Rudnick 1999, Li et al. 2008, Nixon et al. 1981, Pearson et al. 1995a, Rudnick et al. 1994, Winterburn et al. 1989). Steady-state conductive geotherms are pinned to a surface heat flux (mW $m^{-2}$). Crustal and mantle heat production are taken from Rudnick et al. (1998). Adiabatic gradient for a mantle potential temperature of 1,380°C is shown. $T_P$ corresponds to mantle potential temperature.

radioactive heat production of the crust, most of the variation is attributed to thermal boundary layer thickness. Thickness has been estimated to be ~200–250 km beneath cratons and <100 km beneath Phanerozoic terranes (Nyblade 1999, Pollack et al. 1993), although thicknesses exceeding 300 km have also been suggested (Artemieva & Mooney 2001). However, these thickness estimates come with large uncertainties because the assumption of steady state may not be valid, the "measured" surface heat flux may be in error (due to transient effects or to advective components), and the distribution of heat-producing elements in the lithosphere is poorly constrained.

## Constraints from Xenolith Geotherms

Mantle xenoliths provide a direct and model-independent approach in constraining the thermal state of continental thermal boundary layers (Boyd 1987, Rudnick et al. 1998). Because of their rapid ascent rates, their high-pressure and high-temperature equilibrium states are kinetically "frozen in" and preserved in the compositions of the minerals. A variety of thermobarometer pairs have been used to give consistent xenolith geotherms (Brey & Kohler 1990, Ellis & Green 1979, Harley & Green 1982). Xenolith P-T data (**Figure 3**) from the Archean Kaapvaal, Slave, and Siberian cratons define geotherms that intersect the 1,300–1,400°C mantle adiabat at depths between 200 and 250 km. The deepest and hottest xenoliths have historically been referred to as the high-temperature sheared peridotites (see Petrology and Geochemistry of Continental Mantle, below). Xenoliths from the edge of the Archean Tanzanian craton near the active East African Rift fall on a slightly hotter geotherm and limit the local thermal boundary layer to ~150 km (Lee & Rudnick 1999, Rudnick et al. 1994). Proterozoic cratons, such as the Colorado Plateau craton in southwestern North America, also yield thermal boundary layer thicknesses of ~150 km (Smith 2000). Peridotite xenoliths sampled in Phanerozoic terranes are mostly garnet free, so accurate constraints on their pressure cannot be obtained. Nevertheless, the absence of garnet is consistent with lithosphere thicknesses in Phanerozoic terranes that are less than ~60–80 km (depending on the Cr content of spinel; see O'Neill 1981). The thin lithosphere beneath Phanerozoic terranes is corroborated by the depths of magma generation as inferred from the silica activity of the basaltic lavas that host the xenoliths in these regions (Lee et al. 2009).

## Seismic Constraints

Seismic constraints on boundary layer thicknesses give different results depending on the method. Body-wave seismic tomography commonly shows high-velocity anomalies beneath cratons extending to depths beyond 300 km, sometimes as deep as 400 km. These results have long been known to be inconsistent with xenolith geotherms. However, because of the relatively vertical paths of body waves used in tomographic studies, vertical resolution is poor and uncertainties in lithosphere thickness are large.

Surface wave studies provide better depth resolution than body waves in the upper mantle and show that continents are defined by a seismically fast lid underlain by a low-velocity layer, often interpreted to equate with a rheologically weak asthenosphere (Cammarano & Romanowicz 2007, Dalton et al. 2009, Nettles & Dziewonski 2008). Ocean basins have thinner lids (<100 km) than the old cores of continents (~200–250 km). In particular, surface wave anisotropy studies show that cratons are underlain by a layer of radial anisotropy, where horizontally polarized shear waves are faster than vertically polarized shear waves in the depth range of 250–400 km (Gung et al. 2003). This finding suggests that at depths greater than ~250 km, there lies a low-viscosity shear zone (asthenosphere) characterized by lattice-preferred orientation of olivine. Global seismic

attenuation studies based on surface waves also indicate a change in seismic character deeper than ~200 km (Dalton et al. 2009).

Receiver function studies using Sp and Ps converted phases also help constrain lithosphere thicknesses because such conversions are sensitive to sharp subhorizontal velocity transitions (Fischer et al. 2010). For example, Niu et al. (2004) used Ps converted waves to show that the "410"-km discontinuity beneath the Kaapvaal craton was not perturbed. This result, combined with geodynamic constraints on thermal boundary layer thicknesses permitted by a rigid chemical boundary layer, provides an upper bound of <300 km for the thickness of cratons (Cooper et al. 2004). More detailed studies of Sp and Ps conversions within the uppermost mantle are more difficult to interpret (Rychert & Shearer 2009). Sharp velocity gradients occur in Phanerozoic continental regions at depths of <100 km (Rychert & Shearer 2009), consistent with estimates of thermal boundary layer thickness based on surface heat flux, xenolith thermobarometry, and magma thermobarometry (Lee et al. 2009, Luffi et al. 2009, Smith 2000). Beneath cratons, however, Ps and Sp conversions occur at a depth of ~90 km, well within the thermal boundary layer (Rychert & Shearer 2009). The origin of these internal discontinuities is unknown, but dipping structures have been observed in numerous cratons and have been interpreted to represent imbricated oceanic lithosphere or fossilized sutures (Bostock 1999, Hansen & Dueker 2009). Finally, no strong Ps or Sp conversions are seen at the expected base of cratonic thermal boundary layers (see Fischer et al. 2010 for a review). Surface wave studies also do not show universal evidence for the presence of a low-velocity layer beneath cratons (Pedersen et al. 2009). The low-velocity zone beneath cratons may be subtle or even nonexistent, raising the possibility that the low-viscosity layer (e.g., asthenosphere) is very thin beneath continents.

## PETROLOGY AND GEOCHEMISTRY OF CONTINENTAL MANTLE

This section discusses the major- and minor-element chemistry of continental mantle as constrained from xenoliths because these elements control the physical properties of rocks and their petrogenetic origin. Detailed summaries of the petrology and of the trace-element and isotope geochemistry of continental mantle rocks can be found elsewhere in the literature (Canil 2004, Griffin et al. 2003, Griffin et al. 1999, Pearson et al. 2003, Pearson & Wittig 2008, Simon et al. 2007).

### Peridotites

**Peridotites as residues of melt extraction.** Peridotites dominate in continental mantle and consist of olivine, orthopyroxene, clinopyroxene, and an aluminous phase, such as spinel at low pressure and garnet at high pressure (>~2–3 GPa). Owing to differences in continental lithosphere thickness, spinel peridotites and garnet peridotites dominate Phanerozoic mantle and cratonic mantle, respectively. Continental peridotites range from fertile (rich in basaltic melt components) lithologies, akin to "primitive mantle" or pyrolite, to highly melt-depleted lithologies (Boyd 1987, Boyd 1989, Boyd & Mertzman 1987). The former are lherzolitic in composition and characterized by high clinopyroxene mode (10–20%) and high $Al_2O_3$, CaO, and $Na_2O$ content. The latter are harzburgitic (olivine and orthopyroxene) and characterized by low $Al_2O_3$, CaO, and $Na_2O$ and high MgO content.

**Figure 4** shows that $Al_2O_3$ and $Na_2O$ content of Phanerozoic, Proterozoic, and Archean peridotites are negatively correlated with MgO. Because progressive melt extraction results in the depletion of clinopyroxene and garnet, leaving behind an olivine- and orthopyroxene-rich residue, such trends can be broadly explained in terms of melt depletion. Melt depletion also results in

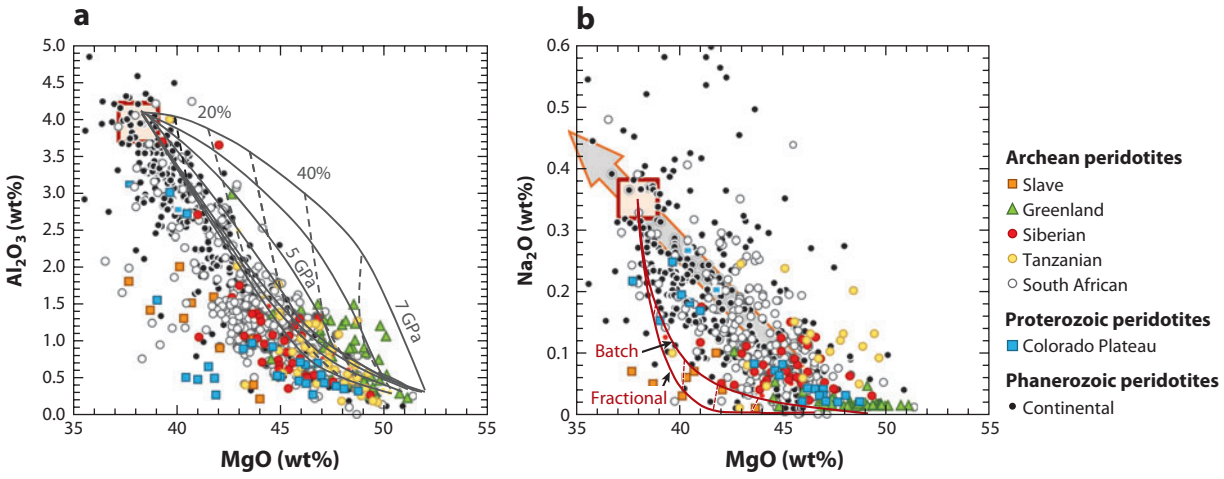


**Figure 4**

Whole-rock peridotite compositions. (*a*) $Al_2O_3$ versus MgO. (*b*) $Na_2O$ versus MgO. Archean and Proterozoic samples pertain to xenolith data from the literature. Phanerozoic continental peridotites pertain to xenoliths and obducted ophiolite terranes described in the literature. In panel *a*, isobaric batch melting curves for different pressures (*solid lines*) are given at 1-GPa intervals from 1 to 7 GPa (Walter 1999); dashed contours indicate melting degrees at 10% intervals. In panel *b*, model curves for isobaric batch (2 GPa) and polybaric fractional melting are given with 10% melting contours; fractional melting assumes adiabatic decompression melting with an initial melting pressure of 2.5 GPa (see Luffi et al. 2009 for details). The large arrow in panel *b* represents a qualitative trajectory for mixing between basaltic liquids and harzburgite. The large square in panels *a* and *b* represents an estimate of the "primitive" mantle (McDonough & Sun 1995).



an increase in olivine/orthopyroxene ratio and atomic Mg# in the residual peridotite [Mg# = atomic Mg/(Mg + $Fe_T$), where $Fe_T$ corresponds to total Fe content]. This occurs because liquids in equilibrium with peridotites have higher $SiO_2$, lower MgO, and lower Mg#. Using Mg/Si as a proxy for olivine mode (atomic Mg/Si $\sim$ 2) and orthopyroxene mode (atomic Mg/Si $\sim$ 1) shows that Mg/Si and Mg# correlate, as predicted from experimental studies on peridotite melting (**Figure 5**). Interpreted in terms of melt depletion, the high Mg/Si and Mg# of many of the Archean peridotites require high degrees of melt extraction compared with Phanerozoic peridotites, which have lower Mg/Si and Mg#. **Figure 6** shows histograms of Mg# for different peridotite suites, ranging from Archean cratons to Phanerozoic xenoliths and obducted ophiolites. Although there are no fundamental differences between Archean and Phanerozoic peridotites in terms of element covariation trends, Archean peridotites consistently have higher Mg# than Proterozoic and Phanerozoic peridotites. These differences have been interpreted to reflect secular changes in the average degree of melting associated with the formation of continental mantle (Griffin et al. 2003).

**Modal metasomatism and refertilization of peridotites.** Major-element systematics, however, cannot be interpreted solely in terms of melt depletion. First, a small group of peridotites, represented primarily by Archean peridotites from the Kaapvaal craton in South Africa, have excess orthopyroxene for a given Mg# and thus deviate from the melt depletion trend toward low Mg/Si shown in **Figure 5** (Boyd 1989). Suggestions for this excess orthopyroxene have included melt-rock reaction between peridotite and silicic melts generated by partial melting of subducting oceanic crust (Boyd 1989, Rudnick et al. 1994, Simon et al. 2007), metasomatism by Si-rich aqueous fluids (Bernstein et al. 1998, Kelemen et al. 1998, Simon et al. 2007, Smith et al.

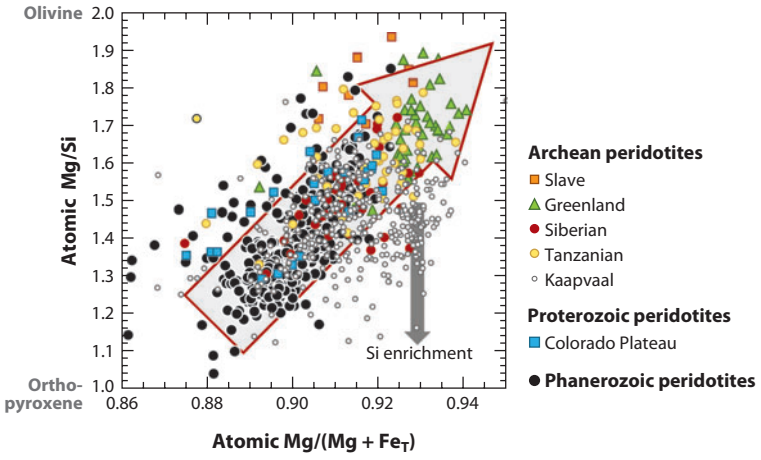


**Figure 5**

Atomic Mg/Si versus atomic Mg/(Mg + $Fe_T$) (also known as Mg#) for peridotites. The large positively sloping arrow represents a trend of melt depletion as constrained by experimental melting of fertile peridotite. With increasing melt depletion, the residue increases in Mg/(Mg + $Fe_T$) and olivine mode (high Mg/Si). Deviations from this trend toward high Si (low Mg/Si) indicate orthopyroxene enrichment (*vertical, downward pointing arrow*).

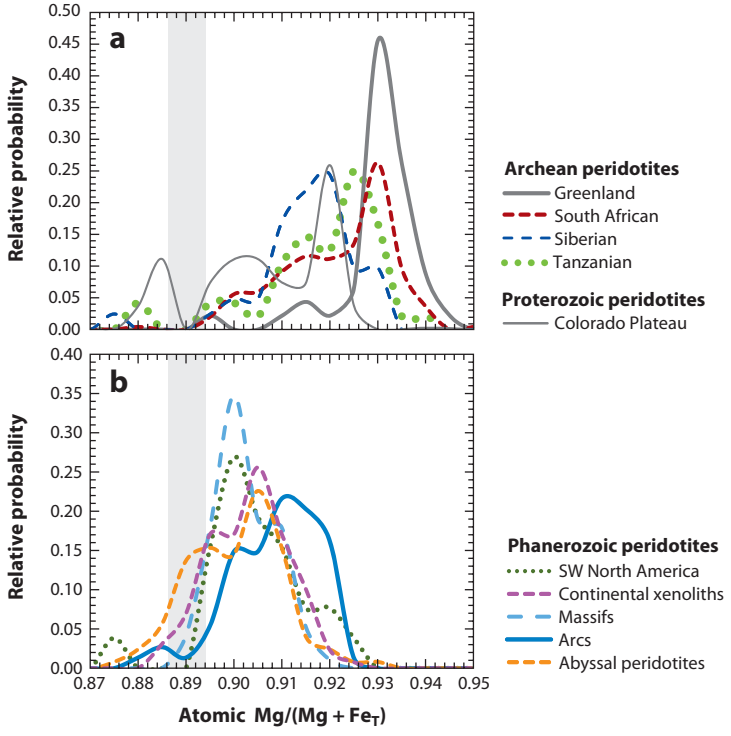


**Figure 6**

Relative probability histograms for whole-rock atomic Mg/(Mg + $Fe_T$) for peridotites from (*a*) Archean and Proterozoic terranes and (*b*) Phanerozoic terranes. Vertical shaded bar represents primitive-mantle value.

1999), addition of orthopyroxene-rich cumulates generated from high-pressure magmas (>7 GPa) (Herzberg 1993), physical segregation of olivine and orthopyroxene during metamorphism (Boyd 1989), and inheritance from serpentinized protoliths (Canil & Lee 2009).

A more serious complication concerns peridotites that have been refertilized (i.e., re-enriched in basaltic melt components) but that adhere to apparent melt-depletion trends in terms of major elements. For example, the negative correlation between $Na_2O$ and MgO appears roughly consistent with melt depletion. However, because $Na_2O$ is incompatible in the residue and MgO is compatible in the residue, melt depletion results in nonlinear trends arising from the efficient extraction of $Na_2O$ (**Figure 4*b***; see Elthon 1992, Luffi et al. 2009). The observed linear $Na_2O$-MgO trends thus suggest binary mixing between two components, a highly melt-depleted peridotite, and a basaltic melt (see also Ionov et al. 2005 and Le Roux et al. 2007). Interestingly, many of the most fertile lithologies are found at the base of the continental lithosphere and have been referred to as the high-temperature sheared peridotites because of their commonly mylonitic fabrics (Boyd 1987). Some of these fertile lithologies preserve ancient unradiogenic $^{187}Os/^{188}Os$ isotopic compositions, suggesting that refertilization was relatively recent (Carlson et al. 2005, Pearson et al. 1995a).

**Temperatures, pressures, and extent of melt extraction.** The above observations indicate that continental mantle is the product of at least two major processes: melt depletion followed by refertilization or other major metasomatic enrichment processes (e.g., Si enrichment). Of interest are the pressures and temperatures over which melt depletion occurred. These quantities have been estimated from comparisons of major-element compositions with partial melting experiments of fertile peridotites. More sophisticated, model-dependent approaches have considered decompression melting; details can be found in Herzberg (2004) and Walter (1999, 2003). A simple and less model-dependent approach is to examine the covariation of FeO and MgO in peridotites (**Figure 7**). FeO in peridotites and coexisting liquids is often used as a pressure indicator, but Fe partitioning is actually significantly more sensitive to temperature than to pressure. The correlation between pressure and Fe in peridotites and liquids is the fortuitous consequence of the peridotite solidus having a positive Clapeyron slope, i.e., $dP/dT > 0$. A simultaneous examination of FeO and MgO can determine the average temperature and degree of melting, $F$, on the basis of a combination of mass balance and the equilibrium relationships of Fe-Mg exchange between peridotite and melt; this process follows the approach of Hanson & Langmuir (1978) (see also Pearson et al. 1995a). As seen from the perspective of the peridotite residue (**Figure 7**), high $F$ is reflected in high Mg# and high MgO, whereas high temperature is reflected in terms of low $FeO_T$. Although secondary re-enrichment processes complicate the interpretation of FeO and MgO, all samples identified as Si enriched using the Mg/Si–Mg# plot (**Figure 5**) define a distinctive low-FeO field and are excluded from discussion. Identifying basalt-refertilized peridotites is not as straightforward, but peridotites with Mg# > 0.92 may be close to pristine as they do not fall on mixing arrays (**Figure 7**).

Archean residual peridotites with Mg# > 0.92 experienced 30–50% melt depletion (relative to a "primitive-mantle" starting composition) at average temperatures between 1,500 and 1,700°C (**Figure 7**), whereas Phanerozoic peridotites show melting degrees of <~30% and melting temperatures between 1,300 and 1,500°C. These temperature estimates are consistent with Archean and Phanerozoic mantle potential temperatures as estimated from the major-element compositions of Archean komatiites and Phanerozoic mid-ocean ridge basalts (Herzberg et al. 2010, Lee et al. 2009). The high temperatures (up to 1,900°C) often cited for cratonic peridotites undoubtedly refer to the Si-rich peridotites, which are FeO poor and hence yield overestimated temperatures.

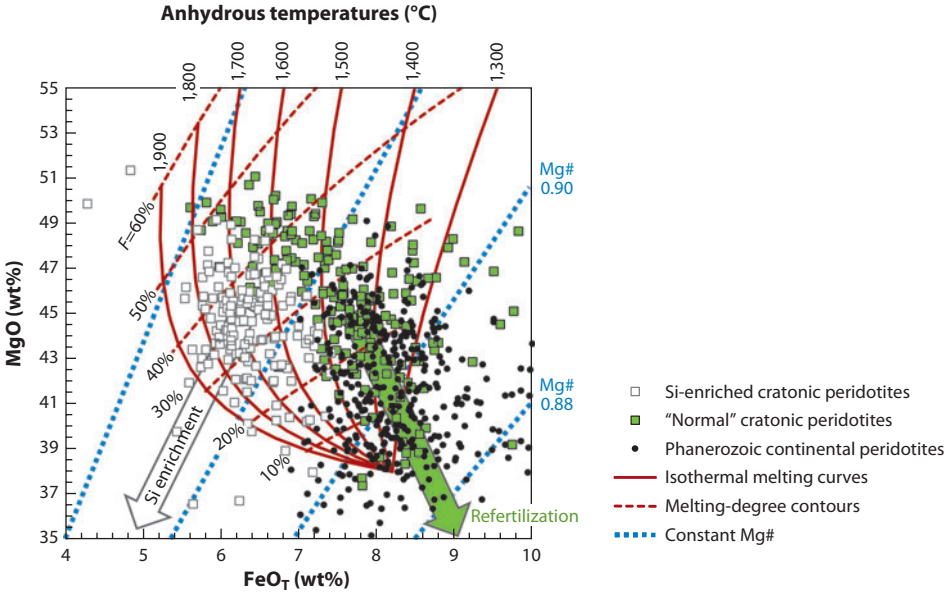


**Figure 7**

Whole-rock $FeO_T$ versus MgO. Squares represent Archean cratonic peridotites: White squares represent Si-enriched peridotites that fall off the Mg/Si–Mg# melt-depletion trend shown in **Figure 5**; green squares represent "normal" cratonic peridotites. Black circles represent Phanerozoic continental peridotites. Red solid lines represent isothermal melting curves (which implicitly assume a change in pressure). Red dashed lines represent melting-degree contours. Blue diagonal lines represent constant Mg#. The white arrow shows the direction of Si enrichment; note no change in Mg#. The green arrow shows the direction of refertilization; note the decrease in Mg#. Calculations assume a given primitive-mantle starting composition, a mass balance for batch melting, and a coefficient of 0.32 for the Fe-Mg exchange between bulk peridotite and melt. Mg of melt is converted to temperature using an empirical relationship between MgO and temperature in olivine-saturated anhydrous melts. *F*, average degree of melting.

Constraints on pressures can also be obtained. Melting at high pressure where garnet is stable on the solidus should yield residues with high $Al_2O_3$ and Yb for a given level of MgO content, but cratonic peridotites follow the same trends in Al-Mg and Yb-Mg space as Phanerozoic spinel peridotites. This suggests that cratonic peridotites largely melted in the absence of garnet and thus at pressures lower (<4–5 GPa) than their present equilibration pressures (3–7 GPa) (Canil 2004, Kelemen et al. 1998, Lee 2006, Pearson & Wittig 2008, Wittig et al. 2008). This is also consistent with the high Cr content in cratonic peridotites, which requires melting in the spinel stability field because Cr is much more compatible in spinel than in garnet (Canil 2004). Counterarguments maintain that most of the melt-depletion history has been erased by refertilization and that extreme degrees of melt depletion completely remove garnet so that Yb and Al contents are no longer diagnostic of pressure (Arndt et al. 2009). However, it is difficult to argue that the high Cr content of cratonic peridotites resulted from refertilization (particularly in the garnet stability field).

Assuming melting occurs by adiabatic decompression, final pressures of melting can be estimated from the intersection of melting-degree contours and the average temperature of melting in P-T space (**Figure 8**). The 1,500–1,700°C and $F = 30$–50% ranges mentioned above suggest that final melt extraction took place between 1 and 5 GPa. Initial pressures of melting were certainly greater but unlikely to have exceeded 7–8 GPa. Bernstein et al. (2007) argued that the near-exhaustion of orthopyroxene and high Mg# in cratonic peridotites require final melt-extraction

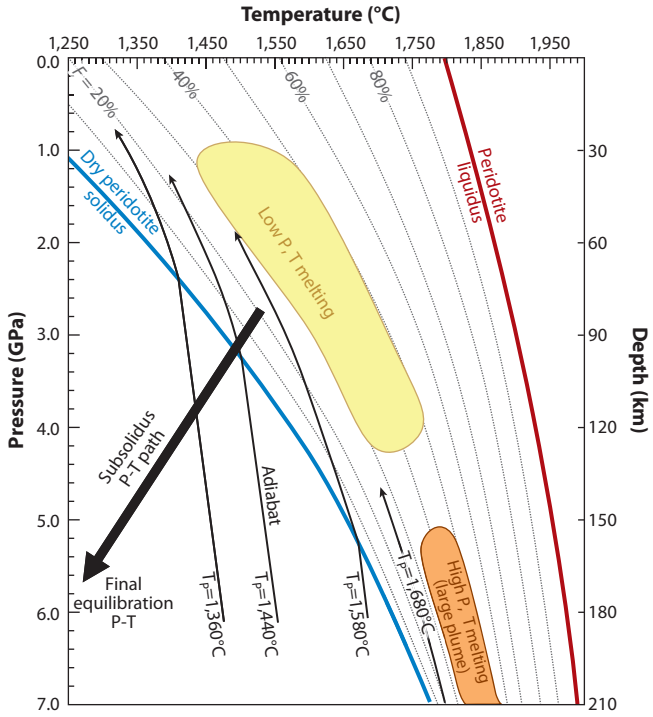


**Figure 8**

Solidus and liquidus of peridotite, showing melting-degree contours (calculated from Katz et al. 2003). Melting adiabats corresponding to solid mantle potential temperatures are given. Yellow-shaded region represents the inferred melting temperature (T) and melting degree of cratonic peridotites as determined from **Figure 7**, which constrains the pressure (P) interval of melting. The arrow connects these melting P-T conditions toward the final (metamorphic) equilibration P-T values of peridotite xenoliths based on xenolith thermobarometry. $T_P$ corresponds to mantle potential temperature.

pressures to be <3 GPa. Collectively, the above observations indicate that cratonic peridotites melted at low pressures (<4–5 GPa) and that afterward, they were tectonically displaced to greater pressures (up to 7–8 GPa). Their current mineralogy is the product of metamorphic reactions taking place during this transit in P-T space (**Figure 8**). Cox et al. (1987), Canil (1991), and Saltzer et al. (2001) also have suggested that most of the garnet in cratonic harzburgites is not magmatic but formed during subsolidus compression, either by exsolution from pyroxenes or at the expense of spinel.

## Pyroxenites

Pyroxenites are the second-most abundant rocks in continental mantle (Barth et al. 2001, 2002; Beard et al. 1996; Fung & Haggerty 1995; Horodyskyj et al. 2007; Jacob 2004; Pyle & Haggerty 1998; Taylor & Neal 1989; Taylor et al. 2003). Many of these pyroxenites contain garnet and are loosely referred to as eclogites. Garnet-bearing pyroxenites also occur in some Phanerozoic peridotite suites. Because of their high densities compared with peridotites, their presence may have profound implications for the stability of continental mantle.

Cratonic garnet pyroxenites can be subdivided into high-MgO and low-MgO suites (**Figure 9**) (Barth et al. 2001, 2002). Although a complete spectrum exists between the two suites,

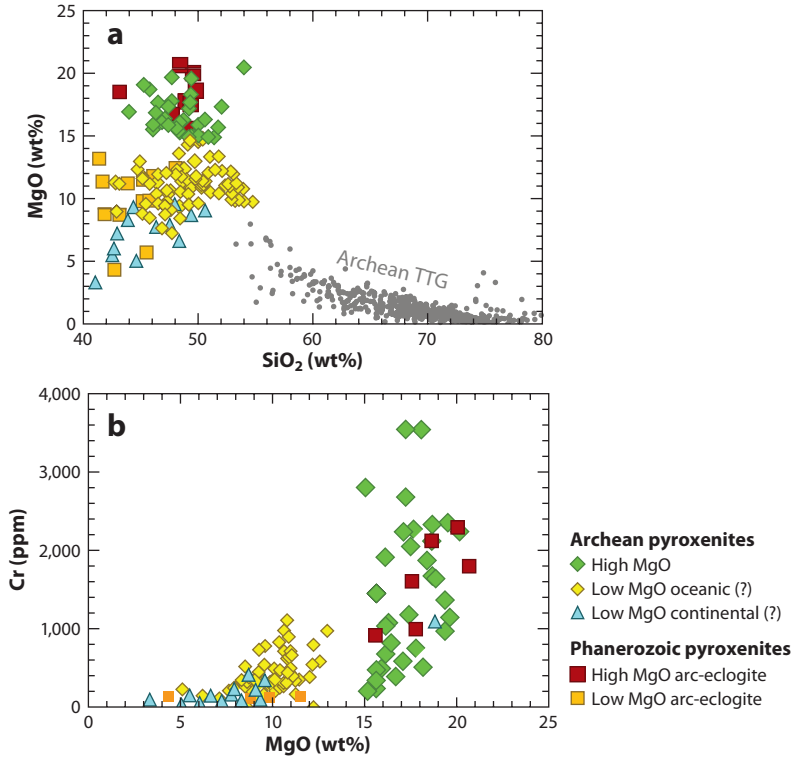


**Figure 9**

Whole-rock geochemistry of garnet pyroxenites from Cretaceous continental arc (Sierra Nevada, California) and Archean cratons (Siberian, South African, west African) (Barth et al. 2001, 2002; Ducea & Saleeby 1998; Fung & Haggerty 1995; Jacob 2004; Lee et al. 2006; Pyle & Haggerty 1998; Taylor et al. 2003). Low-MgO, crustal eclogites from ultrahigh-pressure terranes in China are shown for reference (Song et al. 2003). (*a*) MgO versus $SiO_2$. (*b*) Cr versus MgO. TTG, tonalite-trondhjemite-granodiorite. Data from literature compilations.

we define the demarcation to occur at 15 wt% MgO (Horodyskyj et al. 2007). High-MgO garnet pyroxenites are characterized by clinopyroxene ~ orthopyroxene > garnet modes, high Mg#, and high Ni and Cr content. Low-MgO garnet pyroxenites are dominated by garnet ≥ clinopyroxene, generally minor amounts of orthopyroxene, low Mg#, and low Ni and Cr content. Many of the high-MgO garnet pyroxenites have major-element compositions similar to picritic basalts (high MgO and low $SiO_2$, <50 wt%), but many have $SiO_2$ content too high (50 wt%) to represent basaltic liquids generated from anhydrous partial melting of the mantle. Most low-MgO garnet pyroxenites have major-element compositions broadly similar to modern mid-ocean ridge basalts (MORBs), although $SiO_2$ content may be slightly lower than what is found in MORBs.

**Low-MgO garnet pyroxenites.** Hypotheses for the origin of low-MgO pyroxenites abound. Their protoliths are widely thought to be oceanic crust or gabbros because their oxygen isotopic compositions deviate by >1‰ units (Barth et al. 2001, Jacob 2004) from the canonical mantle value of $\delta^{18}_{SMOW} = 5.5‰$ (Mattey et al. 1994). Only low-temperature alteration is considered efficient in fractionating oxygen isotopes. For example, hydrothermal alteration results in both positive and negative oxygen isotope fractionations within the oceanic lithosphere (positive

deviations in the uppermost crust and negative deviations in the lower crust due to inheritance from $^{18}O$-depleted reactive waters; see Gregory & Taylor 1981). Archean low-MgO pyroxenites often show both positive and negative deviations; hence their protoliths may represent different sections of subducted oceanic lithosphere (see Jacob 2004 for a review). Cratonic low-MgO pyroxenites, however, are actually poorer in $SiO_2$ and $Na_2O$ than Franciscan-type eclogites found in Phanerozoic accretionary wedges; pyroxenites with bona fide MORB protoliths are an example. These differences signify either that the protoliths do not actually resemble modern MORB or that their compositions have been modified by partial melt extraction (Barth et al. 2001, Rollinson 1997). Such melting would generate felsic rocks similar to the tonalite-trondhjemite-granodiorite series rocks commonly found in Archean terranes (Condie 2005, Foley et al. 2002, Rapp et al. 2003, Smithies 2000).

The aforementioned stable-isotope evidence for a low-temperature origin has been challenged on the suggestion that stable-isotope fractionation can, under some conditions (presumably during kinetically limited processes, such as melt-rock reaction), occur at high temperatures (Griffin & O'Reilly 2007). However, such processes have never been demonstrated to be efficient enough to generate >1‰ fractionation or to give rise to systematic correlations between stable isotopes and major lithologic types. Moreover, diamonds with eclogitic inclusions contain sulfides showing mass-independent sulfur-isotope fractionation, a feature that has been documented to occur only during photochemical reactions high in Earth's atmosphere (Farquhar et al. 2002). In addition, diamonds with eclogitic inclusions are made of extremely light carbon, as exemplified by $\delta^{13}_{PDB}C$ values significantly lower (approaching values of –35‰) than the canonical mantle value of –5.5‰ that characterizes diamonds with peridotitic inclusions (Deines et al. 2001). Such low values are generally taken to reflect a biogenic origin, but Cartigny et al. (1998) showed that diamond nitrogen isotopes do not have a biogenic signature. Although there is still room for debate, the consistency of several lines of independent observations (with the exception of N isotopes) has led to general agreement that low-MgO eclogites represent recycled oceanic crust.

**High-MgO garnet pyroxenites.** This suite of pyroxenites is more difficult to interpret. Their oxygen isotopic compositions are mantle-like (Barth et al. 2002). They have been interpreted to represent (*a*) trapped high-pressure, mantle-derived liquids, (*b*) the products of melt-rock reaction between basaltic liquids and peridotite, (*c*) subducted picritic oceanic crust, and (*d*) high-pressure cumulates (Barth et al. 2001, 2002). None of these scenarios is mutually exclusive, but each has different implications for the origin of continental mantle. The major-element compositions of some of these garnet pyroxenites have modern analogs as olivine-plagioclase-pyroxene gabbros in oceanic crust or olivine-rich magmas, such as Hawaiian picrites. However, most are too rich in $SiO_2$ to originate from gabbro or picrite protoliths. High-MgO pyroxenite cumulates from Phanerozoic arcs are a better match in terms of major-element and Ni and Cr content (Ducea & Saleeby 1998, Horodyskyj et al. 2007, Jagoutz et al. 2009, Lee et al. 2006). These similarities to arc-related pyroxenites suggest that it may be worth considering arc magmatism as a factor in the petrogenesis of cratons.

## Cryptic Metasomatism

A pervasive feature of continental mantle peridotites is that their trace-element signatures (and time-integrated radiogenic isotopic compositions) are often overprinted by re-enrichment processes (Roden & Murthy 1985). These processes recall the refertilization and modal metasomatic processes described above, but in many cases the metasomatism is of a cryptic nature, in which trace-element signatures have been modified but the major elements and mineralogy have not

(Bedini et al. 1997, Canil 2004, Ionov et al. 2002, Pearson et al. 2003, Pearson & Nowell 2002, Zindler & Jagoutz 1988). Some notable metasomatic "flavors" are highlighted here. One type is represented by similar enrichments in the high–field strength elements (e.g., Nb, Ta, Zr, Hf, and Ti) and the rare-earth elements. This signature is typical of intraplate magmas, such as alkali basalts, basanites, and ultrapotassic rocks; thus xenoliths with such signatures are often interpreted to have been infiltrated by similar liquids at depth (Dawson 1987). In some cases, enrichments in high–field strength elements are sufficient to stabilize accessory minerals, such as rutile, ilmenite, and zircon (Dawson & Smith 1977, Rudnick et al. 1999), in which case metasomatism is modal, not cryptic. Such metasomatism can also introduce hydrous minerals, such as phlogopite and amphibole, and can increase Fe oxidation state (Dawson & Smith 1977).

Another type of metasomatism is represented by depletions in high–field strength elements relative to the rare-earth elements and thought to derive from volatile-rich fluids (e.g., hydrous or carbonatitic fluids) because the solubility of these elements is much lower in fluids than in large-ion lithophile elements and light rare-earth elements (Kelemen et al. 1993). In intraplate environments, these signatures are commonly attributed to carbonatite metasomatism (Dautria et al. 1992, Ionov et al. 1993, Rudnick et al. 1993, Yaxley et al. 1991), but in some cases subduction-zone fluids may have been involved (Lee 2005). What these trace-element-enriched peridotites hold in common is that the responsible metasomatizing agent was most likely a low-degree melt.



## INTERNAL STRUCTURE OF CONTINENTAL MANTLE

### Compositional Stratification

**Figure 10** plots whole-rock Mg# of peridotites as a function of equilibration depth for several Archean cratons and one Proterozoic craton. The Archean Siberian (Boyd et al. 1997), Kaapvaal (Boyd & Mertzman 1987, Boyd et al. 1993, Simon et al. 2007, Winterburn et al. 1989), and Slave (Canil 2008, Kopylova & Russell 2000, Kopylova et al. 1999) cratons show highly depleted (high-Mg#) peridotites in the upper ~150 km but more fertile lithologies at greater depths. In particular, at depths shallower than 150 km for the Siberian and Kaapvaal cratons, there is no systematic covariation of melt depletion with depth. However, in the Slave craton, peridotite fertility increases progressively with depth (Kopylova & Russell 2000). The Archean Tanzanian (Lee & Rudnick 1999, Rudnick et al. 1994) and Proterozoic Colorado Plateau (Ehrenberg 1982, Lee et al. 2001, Smith 2000) cratons show relatively restricted xenolith equilibration pressures, but this most likely arises from sampling bias of the host magmas. More curiously, the Tanzanian and Colorado Plateau xenoliths show a complete spectrum between fertile and highly melt-depleted peridotites at a given depth. A nagging question is whether xenolith demographics are representative of the mantle's true stratigraphy, as the sampling characteristics of kimberlites and other host magmas are not well understood. To decrease sampling bias, Griffin et al. (2003) reconstructed mantle stratigraphic sections from thousands of xenocrystic peridotite minerals resulting from disaggregation of xenoliths during magmatic ascent. The whole-rock stratigraphy is broadly consistent with the Griffin et al. (2003) xenocryst results in that cratons are dominated by highly melt-depleted peridotites at depths shallower than ~150 km, but more fertile and metasomatized lithologies dominate at greater depths. On the basis of the geochemical and isotopic data discussed above, this fertile layer appears to originate from melt-depleted peridotites via refertilization rather than represent undepleted mantle.

### Density Structure

The compositional stratigraphy has implications for the density structure of continents. Although there is no perfect parameterization of density as a function of composition, there is a general

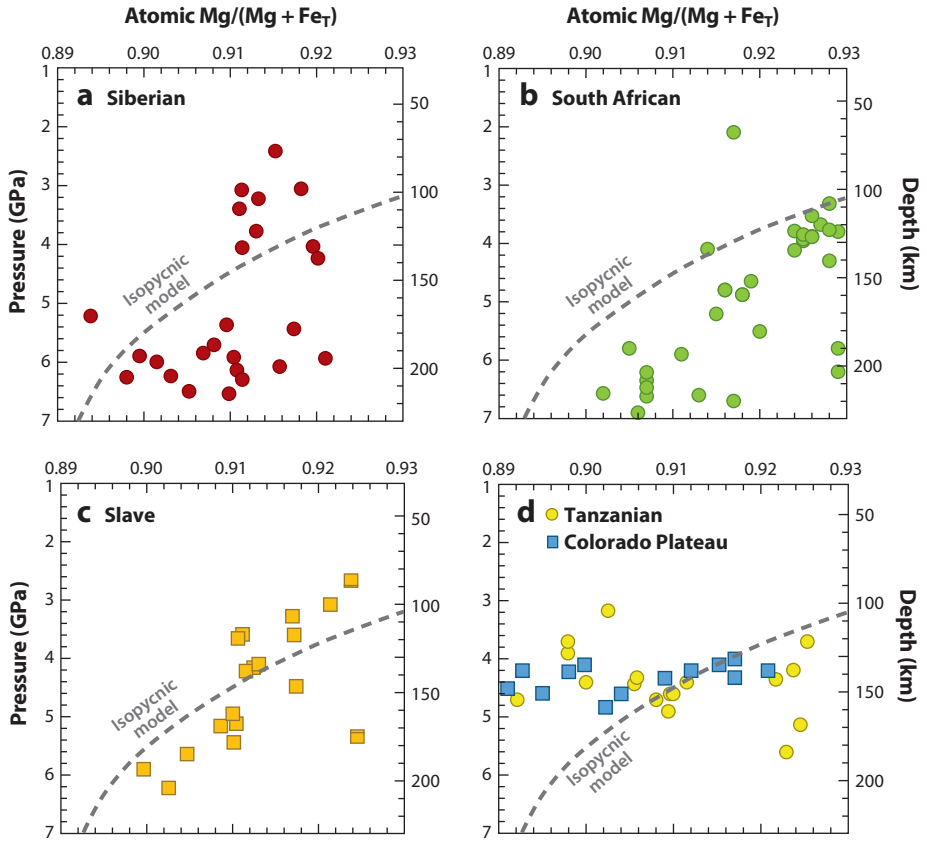


**Figure 10**

Mg# [atomic Mg/(Mg + Fe$_T$)] of cratonic peridotites versus depth for (*a*) the Siberian craton, (*b*) the South African craton, (*c*) the Slave craton, and (*d*) the Tanzanian and Colorado Plateau cratons. Lines labeled isopycnic represent the hypothetical Mg# needed to make cratonic mantle compositionally buoyant enough to exactly compensate for the negative thermal buoyancy at every depth. Craton thermal states taken from xenolith geotherms in **Figure 4**. Conversion of Mg# to density uses parameterizations from Lee (2003).

decrease with increasing Mg# (Jordan 1979, Lee 2003, Schutt & Lesher 2006). An increase in Mg# from 0.89 to 0.93 yields a ∼2% density decrease. Cratonic mantle is on average ∼500–700°C cooler than the ambient mantle (∼1,400°C), resulting in a ∼2% increase in density due to thermal contraction. Thus density variations associated with melt depletion are of the same but opposite magnitude as thermal buoyancies. Using the density-Mg# relationship of Lee (2003), $\rho = -1.44\text{Mg\#} + 4.66$, and the xenolith geotherms shown in **Figure 4**, we plot how Mg# would vary with depth if the perfectly isopycnic conditions required by the tectosphere hypothesis were met (**Figure 10**). Perfectly isopycnic conditions require Mg# to decrease with depth gradually (**Figure 10**). Such a trend is seen only in the Slave craton. Although the Kaapvaal and Siberian cratons do not show perfect isopycnic density structure, their mantles overall are neutrally buoyant to within error. Kaapvaal cratonic peridotites may even be offset by +0.01 Mg# units from isopycnic conditions. This would correspond to an excess compositional buoyancy of ∼0.4%. These excess chemical buoyancies, based on peridotites alone, have previously been suggested (Kelly et al. 2003), but given the lack of free-air gravity anomalies over continents, there should be no

excess buoyancies. Kelly et al. (2003) suggested that dense garnet pyroxenites could account for the missing buoyancy. Garnet pyroxenites are 2–12% denser than peridotites (Horodyskyj et al. 2007). An excess peridotite buoyancy of 0.4%, if real, would require 3–8% of low-MgO garnet pyroxenites (5–12% denser than peridotite) or 8–20% of high-MgO garnet pyroxenites to make up the difference. Incidentally, the 3–8% of low-MgO garnet pyroxenites is broadly consistent with the proportions of low-MgO garnet pyroxenites observed in garnet xenocryst populations in kimberlites (Schulze 1989).

Garnet pyroxenites may have distinct seismic signatures. Low-MgO garnet pyroxenites have P- and S-wave velocities 1% and 1–3% higher than peridotite, respectively, which are sufficient to generate distinctive reflectors or converted phases (Horodyskyj et al. 2007, Levander et al. 2005). Dipping or subhorizontal structures of this type have been observed in the Slave, Wyoming, and possibly the Kaapvaal cratons and have been interpreted to represent the tops of fossil oceanic lithosphere (Bostock 1999). High-MgO pyroxenites, in contrast, have similar or lower P- and S-wave velocities compared with peridotites (Horodyskyj et al. 2007). Their presence could be difficult to detect seismically, but if they occur as a distinct layer within the mantle, they may generate the appearance of a localized low-velocity zone. This would perhaps provide one explanation for the origin of internal discontinuities seen by Rychert & Shearer (2009).

## Water Content and Viscosity Structure

Understanding the water budget of continental mantle is important because the viscosity of olivine, which dominates the rheology of peridotite, decreases substantially in the presence of minute amounts of bound H (Hirth & Kohlstedt 1996). Because H is highly incompatible in solids during partial melting (Aubaud et al. 2008), the highly melt-depleted peridotites of cratons are expected to be dehydrated and intrinsically strong (Hirth et al. 2000, Pollack 1986). The database for H in nominally anhydrous minerals—such as olivine, clinopyroxene, and orthopyroxene—is growing, but interpretations of the data are often not straightforward (see Peslier 2010 for a comprehensive review). Because of the high diffusivity of H in these minerals, the measured H content of xenolith-hosted minerals may not be representative of the pre-eruptive state (Kohlstedt & Mackwell 1998, Mackwell & Kohlstedt 1990). A peculiar observation is that despite similar diffusivities, pyroxenes appear to retain H even if coexisting olivines show H loss (Grant et al. 2007, Li et al. 2008, Peslier 2010, Yang et al. 2008).

The pre-eruptive H content of olivines can be retrieved via the assumption of equilibration between olivine and pyroxene (**Figure 11**). Clinopyroxenes from Kaapvaal peridotite xenoliths have clinopyroxene $H_2O$ (Grant et al. 2007, Peslier 2010) corresponding to olivine $H_2O$ content (2–18 ppmw; by weight) that overlaps or falls slightly below that inferred for olivine in the MORB mantle source (~10–30 ppmw; see Hirschmann 2006). Thus these clinopyroxenes are not particularly dry compared with the convecting mantle. Calculated olivine H content from the North China craton (Yang et al. 2008) is mostly drier than MORB olivine and overlaps the low $H_2O$ content of olivines in abyssal peridotite (Peslier et al. 2007), which are thought to be the melting residues of oceanic crust formation. Clinopyroxenes from the Proterozoic Colorado Plateau craton (Li et al. 2008) are the "wettest" cratonic clinopyroxenes measured so far and would correspond to olivine $H_2O$ content equal to or higher than the MORB source. Phanerozoic continental mantle in western North America shows intermediate water content (Grant et al. 2007, Li et al. 2008).

Some samples of cratonic and oceanic lithospheric mantle appear to be dry; this finding is consistent with magnetotelluric studies of several cratons and oceanic lithosphere, which reveal thick, highly resistive layers (Eaton et al. 2009, Hirth et al. 2000). However, many Phanerozoic

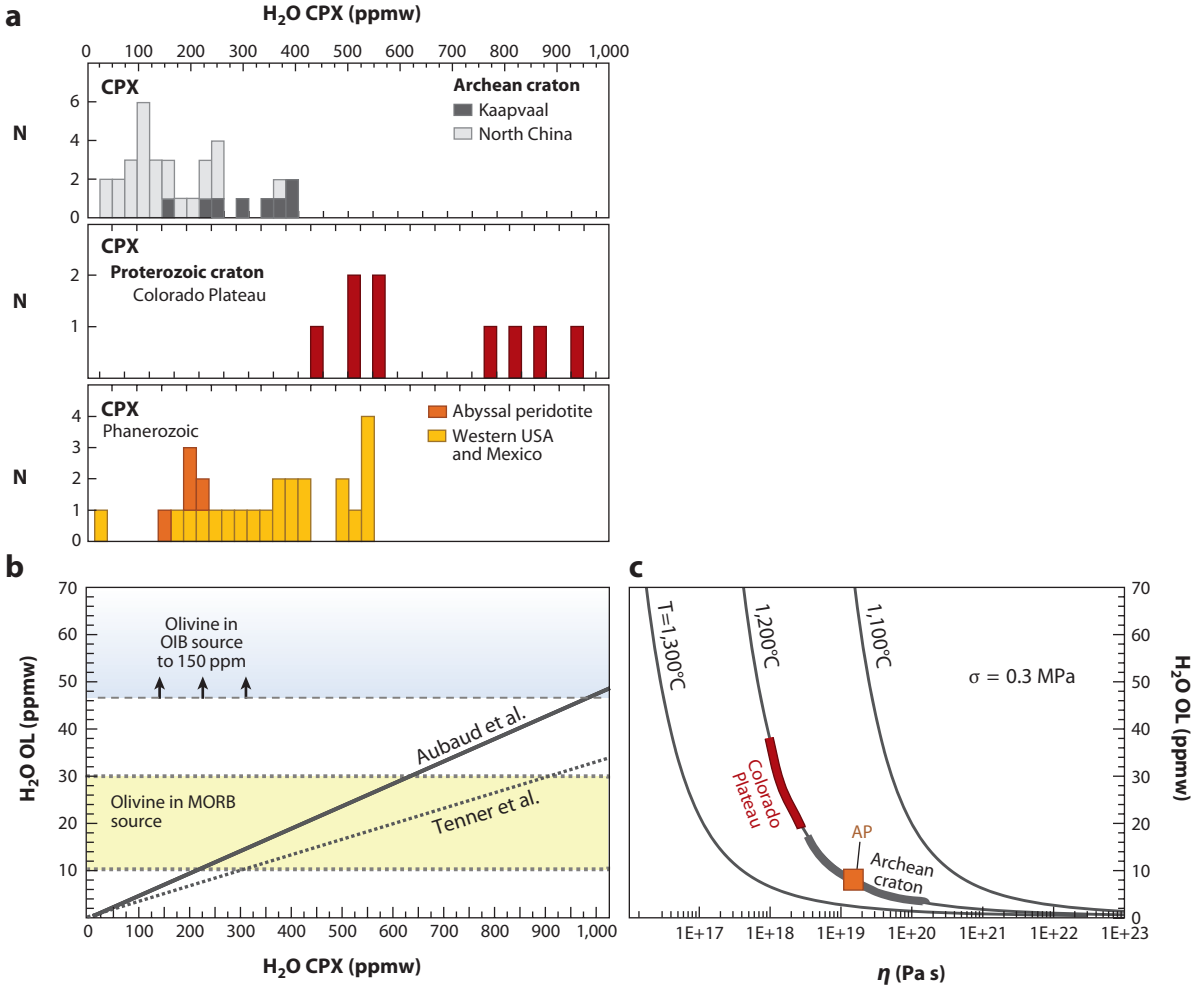


**Figure 11**

Water in continental mantle. (*a*) Bound water in ppm by weight (ppmw) in clinopyroxenes from peridotites of different ages and tectonic environments (Grant et al. 2007, Li et al. 2008, Peslier 2010, Peslier et al. 2007, Yang et al. 2008). (*b*) Water in olivine predicted from olivine/clinopyroxene partition coefficients (Aubaud et al. 2008, Tenner et al. 2009). Fields for water in olivine inferred for the mantle source of mid-ocean ridge basalt (MORB) and ocean island basalt (OIB) were calculated using data from Hirschmann (2006) and the above mineral/mineral partition coefficients. (*c*) Effective viscosity as a function of water content (in ppm by weight) and temperature following procedures in Li et al. (2008) based on modifications of Bai & Kohlstedt (1993) and Mei & Kohlstedt (2000a,b); a background stress state ($\sigma$) of 0.3 MPa is assumed. Abbreviations: AP, abyssal peridotite; CPX, clinopyroxene; N, number of measurements; OL, olivine.

peridotites and cratonic regions that have been influenced by Phanerozoic subduction appear to be "wet." Whether this "wetness" is a primary (e.g., ancient) feature or whether it represents rehydration of an initially dehydrated layer is debated. The possibility of recent rehydration related to kimberlite genesis must also be considered.

In any case, the inferred variations in olivine water content translate into a contrast in effective viscosity of two orders of magnitude. This effect can be seen in **Figure 11*c***, which shows viscosity as a function of water content in olivine using a non-Newtonian flow law [the calculations follow

the approach in Li et al. (2008) using modified flow laws and parameterizations from Mei & Kohlstedt (2000a,b) and Bai & Kohlstedt (1993)]. If continental chemical boundary layers are indeed dehydrated, then continents are also underlain by a compositionally defined rheological boundary layer.

## BUILDING CONTINENTAL MANTLE

We consider the following statements about continental mantle to be robust:

1. Continents, particularly Archean cratons, are underlain by thick thermal boundary layers chemically isolated from the ambient mantle for long time periods.
2. The age spectra of continental crust and mantle are not uniform.
3. Continental mantle is represented by a chemical boundary layer made up of melt-depleted peridotites, ranging from 30–50% melt extraction beneath Archean cratons to <30% beneath Phanerozoic continents.
4. The integrated compositional buoyancy of continental mantle roughly offsets its negative thermal buoyancy, but perfectly isopycnic conditions are not met.
5. The protoliths of cratonic peridotites melted at pressures shallower than their final equilibration pressures.
6. Low-MgO garnet pyroxenites (and associated diamonds) retain signatures of low-pressure, low-temperature processes.

Cratonic mantle may have also been dehydrated during melt extraction. If so, the chemical boundary layer beneath continents may also coincide with a rheologically strong boundary layer. Viable models of generating thick, buoyant, and strong chemical boundary layers must satisfy all the above characteristics. Successful models should also consider possible relationships between the formation of continental mantle and the formation and differentiation of continental crust.

### Plume Origin

One mechanism for cratonic mantle formation is via melting within a large thermal plume (**Figure 12*a***) wherein the high temperatures would lead to high degrees of melting

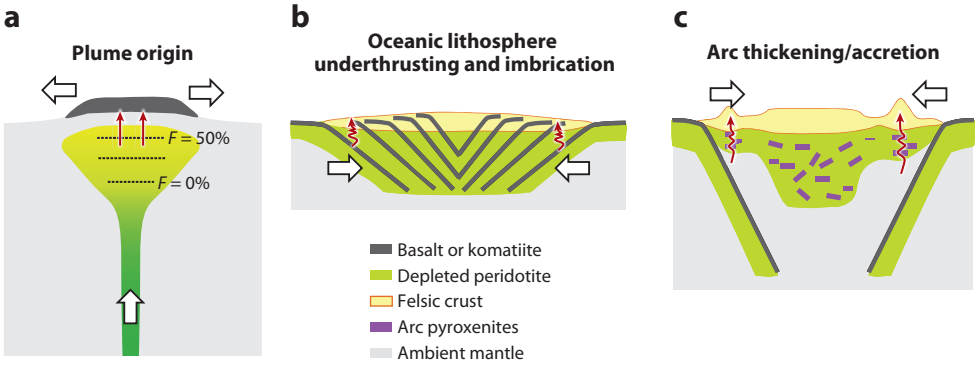


**Figure 12**

Different models for making continental mantle: (*a*) plume origin, (*b*) oceanic lithosphere underthrusting and imbrication, and (*c*) arc thickening/accretion. *F*, average degree of melting. Red arrows indicate partial melt extraction. White arrows indicate directions of motion. Green to yellow shading in panel *a* is a qualitative representation of the degree of melting.

(Arndt et al. 2009, Griffin & O'Reilly 2007, Griffin et al. 2003, Herzberg 1993). The attraction of this model is that a highly melt-depleted, dehydrated, and low-density chemical boundary layer is an immediate product of plume melting, resulting in the formation of a craton from the outset. In other words, this is an in situ formation event: Mantle-crust differentiation and continent formation coincide in space and time. Modern analogs of generating depleted chemical boundary layers by melting in plume heads may be represented by oceanic plateaus, such as Ontong Java. If Archean plumes represent major mantle upwellings, cratonic mantle formation would be expected to be episodic, consistent with the episodic age distribution of continents. Hot-mantle potential temperatures in the Archean would presumably favor cratonic mantle formation by plumes, but the lack of cratons older than 3.5 Ga would imply that early Archean cratons were destroyed.

Specifically, the plume model predicts a gradual stratification from highly melt-depleted (high *F*, Mg#) peridotite at shallow depths to fertile peridotites (low *F*, Mg#) at the base of the thermal boundary layer, but such stratification is not a general feature of cratons (**Figure 10**). This model predicts high-degree melting at a depth of ~200 km, but the 1700°C temperatures of melting recorded by cratonic peridotites are not high enough to generate extensive melting at these depths. Cratonic peridotites have a subsolidus history of pressure increase, and this cannot be explained by the plume model.

## Underthrusting and Imbrication of Oceanic Lithosphere

Another mechanism for building thick continents involves underthrusting or imbrication of oceanic lithosphere (Canil 2004, Canil 2008, Helmstaedt & Schulze 1989, Lee 2006, Pearson & Wittig 2008, Simon et al. 2007). This model (**Figure 12*b***) can explain the low-pressure protoliths of cratonic peridotites, the low-temperature protoliths of low-MgO garnet pyroxenites, the light carbon isotopic signature of eclogitic diamonds, the general lack of systematic compositional stratification with depth, and the presence of subhorizontal and dipping discontinuities within the continental mantle. Partial melting of underthrusting oceanic crust could generate felsic magmas such that formation of evolved continental crust and thick continental mantle would be tectonically linked. Indeed, melting of oceanic crust has been suggested to be an important process in forming the tonalite-trondhjemite-granodiorite suites commonly found in Archean continental crust.

Subtle inconsistencies and questions remain about the model's physical plausibility. This process is thought to be unlikely because negatively buoyant oceanic lithosphere should subduct instead of subcrete (Arndt et al. 2009). However, several lines of evidence indicate that fragments of the Farallon oceanic plate appear to have been captured beneath western North America during the Cenozoic (Luffi et al. 2009, Saleeby 2003). Although the detailed mechanisms have not been worked out, it is clear that plate capture was related to low-angle subduction, perhaps due to changes in relative plate motions, subduction of young lithosphere, or subduction of a buoyant oceanic plateau (Dickinson & Snyder 1978, Saleeby 2003). Thicker and hence more buoyant oceanic crust was probably more common in the hot Archean, so plate capture may have been more efficient in the Archean.

Buoyancy considerations alone constitute only part of the story. Imbrication of oceanic lithosphere must be accommodated by large-scale weak zones or fault planes. Yet, the longevity of continental lithosphere suggests that continental mantle is inherently strong. For imbrication to be viable, these large-scale weak zones must eventually heal (i.e., strengthen) but survive long enough for sufficient underthrusting to generate a chemical boundary layer that is 200–250 km thick (Cooper et al. 2006). Lee et al. (2008) proposed that the serpentinized tops of oceanic mantle may have served as the weak zones. They suggested that the early Archean mantle was too hot for

serpentinites to form and that the period from the late Proterozoic to the present was too cold for the faults to heal. Instead, they showed that the conditions for craton formation by imbrication were favored in the mid-Archean to the early Proterozoic. Whereas the plume model attributes the lack of early Archean cratons to preferential recycling, the lithosphere-imbrication model attributes it to the unfavorable conditions of craton formation during the early Archean. Finally, another difficulty in the imbrication model is that the predicted amount of eclogite exceeds the present amount in the continents (Schulze 1989); thus some mechanism is needed to remove the eclogites *without* simultaneously removing their peridotitic counterparts (see below). Alternatively, if the lower crust is weak, it is possible that much of it would not have been underthrusted.

### Accretion and Orogenic Thickening of Arcs

One driver of Phanerozoic continental-crust formation is the formation of basaltic island arcs followed by accretion and maturation into continental arcs (**Figure 12*c***) (Şengör et al. 1993). Could arc processes have been involved in forming cratons (Kelemen et al. 1998, Parman et al. 2004)? For an arc-origin model to be successful, thickening of arc mantle must occur as discussed above. Young arcs are typically under extension, but as subduction zones mature, arcs often evolve into a compressional state as exemplified by the Cretaceous North American Cordilleran and active Andean continental arcs, wherein arc magmatism coincides with lithospheric thickening (DeCelles et al. 2009, Kay et al. 2005). Some similarities exist between rocks from modern continental arcs and xenoliths from ancient continental lithosphere. For example, the garnet-bearing mafic residues and cumulates generated within the lower crust and mantle of continental arcs (Ducea & Saleeby 1998, Jagoutz et al. 2009, Kay et al. 2005, Lee et al. 2006) are remarkably similar in composition to high-MgO garnet pyroxenites in cratons (**Figure 9**). Archean tonalite-trondhjemite-granodiorite series are geochemically similar to calc-alkaline rocks associated with continental arcs (Chamberlain et al. 2003). Finally, spinels from Archean cratonic peridotites have high Cr/(Cr + Al), a feature that seems to be found primarily in arc environments where hydrous fluxing is thought to promote the high-degree melting necessary to generate high Cr/(Cr + Al) (Arai & Ishimaru 2008). **Figure 13** compares Cr/(Cr + Al) and Mg/(Mg + $Fe^{2+}$) of spinels from subarc mantle (Arai & Ishimaru 2008), abyssal peridotites (Dick & Bullen 1984), Cretaceous Sierra Nevada arc lithosphere in California (E.J. Chin, unpublished data), and the Archean Tanzanian craton (Lee & Rudnick 1999). These lithological similarities make the arc hypothesis attractive, but further testing will require integrating geologic field relationships with petrological and geochemical studies of the crust and mantle.

## DESTROYING CONTINENTAL MANTLE

Although continents appear to be long-lived, many continents may have already been destroyed and recycled, leaving no trace of their prior existence. Geochemical studies of ocean island basalts using radiogenic isotopes as tracers have identified isotopic endmembers that have been interpreted to represent pods of recycled ancient continental mantle in the convecting mantle (Hofmann 1997). More direct evidence comes from using xenoliths, magmas, and geophysics to constrain how the thickness and composition of continental lithosphere change with time. For example, changes in magma geochemistry and Os isotopic composition of lithospheric mantle xenoliths beneath the Archean North China craton suggest Paleoproterozoic lithospheric removal in the north and Phanerozoic lithospheric removal in the east (Gao et al. 2002, Griffin et al. 1998, Menzies et al. 2007, Rudnick et al. 2004). Mesozoic or Tertiary thinning of the Archean Wyoming cratonic mantle has also been suggested on the basis of diamond-bearing kimberlites in the Paleozoic

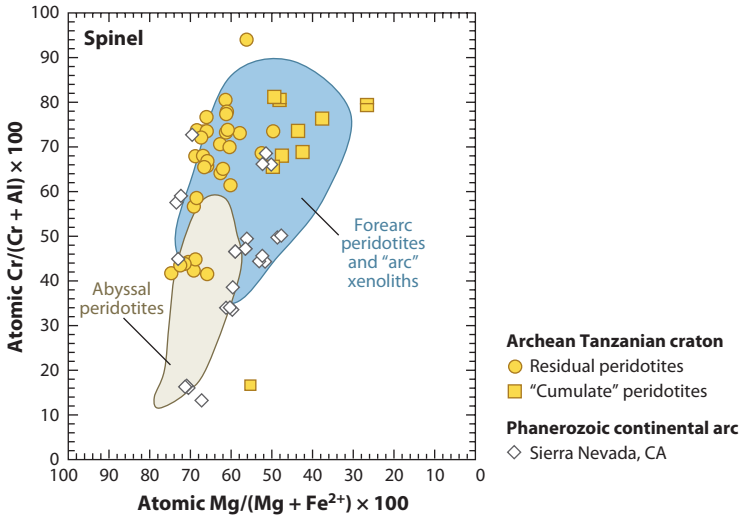


**Figure 13**

Atomic Cr/(Cr + Al) versus atomic Mg/(Mg + $Fe^{2+}$) in spinels from Archean Tanzanian cratonic peridotites (Lee & Rudnick 1999) and peridotite xenoliths from beneath the Cretaceous Sierra Nevada batholith in California (E.J. Chin, unpublished data). Fields for subarc mantle and abyssal peridotites are taken from Arai & Ishimaru (2008) and Dick & Bullen (1984).

and the presently thinner, seismically defined root (Carlson & Irving 1994, Eggler et al. 1988, Goes & van der Lee 2002). Other examples of the recycling of Proterozoic and Phanerozoic continental mantle include the recent removal of Proterozoic and younger lithosphere that has been suggested for Sierra Nevada, California (Ducea & Saleeby 1996, Saleeby et al. 2003); the Proterozoic Colorado Plateau in the southwestern United States (Li et al. 2008); and the Alboran Sea in the western Mediterranean (Seber et al. 1996). Deep removal of Phanerozoic lithosphere has also been suggested for Tibet and many other orogenic belts. Below, we review models for removal of continental lithosphere (**Figure 14**). We do not discuss gravitational or active extensional processes as these processes do not return mantle lithosphere into the convecting mantle.

## Convective Removal

Any lithospheric removal driven by thermal or chemical buoyancy forces (e.g., density-driven forces) is referred to as convective removal (**Figure 14*a***). In the absence of any compositionally induced stabilizing effects, density contrasts are the inevitable consequence of thermal contrasts, and the degree to which buoyancy forces exceed resisting forces (e.g., friction) defines the rate and nature of convective removal. Both vertical and lateral temperature contrasts are capable of driving small-scale convective instabilities, promoting lithospheric erosion from below (growth of Rayleigh-Taylor instabilities; see Huang et al. 2003 and Korenaga & Jordan 2003) and from the sides (edge-driven convection; see King 2005). Such processes may be operating on the edges of the Colorado Plateau and Wyoming and Tanzanian cratons, all of which are surrounded by incipient rifts. Larger-scale instabilities can occur if there is a large overstep in buoyancy forces, such as when a thermal boundary layer is rapidly thickened (compared with thermal relaxation times) during continent-continent collisions (Conrad & Molnar 1997, Houseman & Molnar 1997, Molnar et al. 1998). Such scenarios may result in well-defined convective downwellings, which not

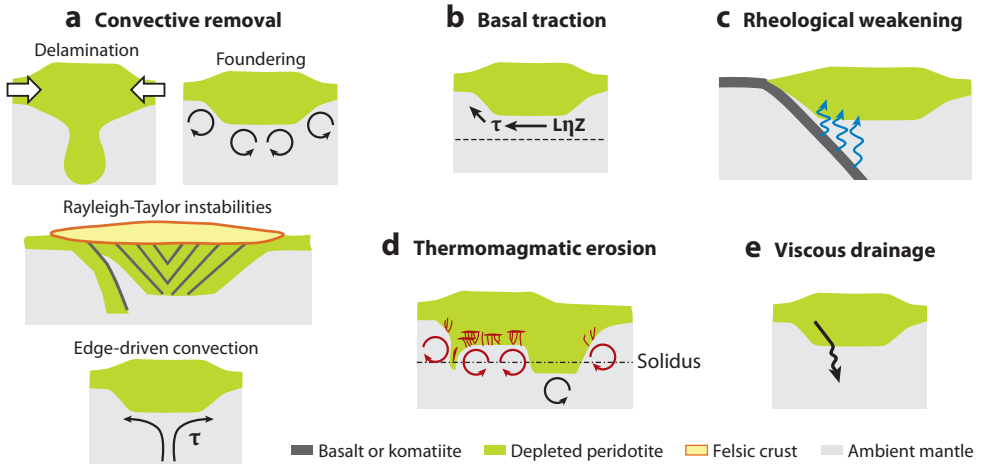


**Figure 14**

Different models for destroying or recycling continental mantle. (*a*) Convective removal, whereby removal is driven by buoyancy forces (thermal or chemical). These processes include delamination, foundering, Rayleigh-Taylor instabilities, and edge-driven convection. (*b*) Basal traction, whereby basal shear stresses drive deformation. This traction is related to the presence of a thinner low-viscosity zone (LηZ) beneath continents. The dashed line represents the base of the low-viscosity zone. (*c*) Removal facilitated by rheological weakening, whereby the rheology of the cratonic mantle is decreased, making it easier for convective or traction-driven removal of lithosphere. (*d*) Thermomagmatic removal, a variant of convective removal. In this mechanism, melts generated below the continental mantle intrude into the continent, increasing its density and temperature, thereby expediting convective removal. This process is suppressed beneath continents with thick roots because the head space for decompression partial melting is substantially reduced. (*e*) Viscous drainage, wherein low-viscosity pyroxenites slide out along an inclined plane over long geologic time periods. Blue arrows represent hydrous fluids derived from a subducting oceanic plate. Black- and red-arrowed circles represent small-scale convection; red-arrowed circles represent convective systems that occur at depths shallower than the solidus and therefore generate partial melts. $\tau$, shear stress.

only are large enough to be detected seismically but also lead to dynamic topography. Lithosphere removal beneath the North China craton could have been triggered by a collisional event (Menzies et al. 2007).

## Basal Traction

Erosion of continental lithosphere can be driven by basal shear stresses imposed by mantle flow in the asthenosphere (**Figure 14*b***). Basal shear stress should increase as asthenosphere thickness decreases. If the bottom of the asthenosphere is defined globally at a relatively constant depth, then asthenosphere thickness should vary inversely with lithosphere thickness. This process has been proposed as a mechanism of limiting craton thickness (Cooper & Conrad 2009), but complete destruction of cratons is unlikely because the shear stresses decrease rapidly as craton thickness decreases.

## Rheological Weakening

Weakening the rheology of continental mantle can facilitate convective removal (**Figure 14*c***). One way to weaken continental mantle is to rehydrate it, perhaps via the infiltration of hydrous

melts or supercritical fluids released from a subducting slab. Both the North China craton and western North America were once underlain by a subducting slab. In western North America, there is growing evidence that much of the lithosphere was modified by hydrous fluids from the "flat"-subducting Farallon plate (Humphreys et al. 2003, Lee 2005, Li et al. 2008, Rowe & Lassiter 2009, Smith 2010) and that this may have weakened the North American lithosphere (Li et al. 2008). Carbonatite metasomatism, which is common in cratonic environments, may also transport water into continental mantle (Dasgupta et al. 2007).

### Thermomagmatic Erosion

Refertilization (in a major-element sense) via diking or porous flow, as suggested by Foley (2008), may be another mechanism of destabilizing continental mantle (**Figure 14*d***) because of the resulting increases in Fe content, water content, and temperature, the latter due to advection of heat (short-term response) and increased heat production (long-term response). The increases in Fe and water content lead to compositional densification and a decrease in viscosity, promoting convective removal. However, refertilization is effective only if sufficient amounts of silicate melts are generated (low-degree melts, such as carbonatites, are too minor to lead to any fundamental changes in major-element composition). Both plume impingement and small-scale convective instabilities are favorable environments for generating melts, provided that the mantle solidus is crossed during decompression, but adequate head space for decompression above the solidus is required for melting. Thermomagmatic erosion should thus be more efficient beneath thin continents than beneath thick continents, where it may not operate at all unless thermal plumes or anomalous radiogenic heat production locally raise potential temperature. We speculate that this could explain why thick Archean cratons are relatively undisturbed, whereas thinner Phanerozoic and Proterozoic continents show more evidence for convective thinning. If so, the fate of continents may in part be related to their initial thicknesses.

### Viscous Drainage

We suggest that inclined layers of garnet pyroxenite could "drain" back into the convecting mantle owing to their high densities and low viscosities compared with peridotite (**Figure 14*e***). Drain rates could range from a few tens to hundreds of millions of years; the rates would correlate positively with density contrast, dip angle, and the square of pyroxenite layer thickness and inversely with viscosity of the pyroxenite. This scenario, albeit untested, provides a mechanism for removing garnet pyroxenites from the continental mantle without disturbing the peridotite framework of the continent.

## FUTURE DIRECTIONS

Numerous outstanding questions are not addressed here. What is the petrogenetic connection between continental crust and continental mantle? How do continental boundary layers influence global convection and heat loss from Earth? What role do thick chemical boundary layers play in modulating timescales of supercontinent breakup and assembly? How do continents modulate the nature and style of intraplate magmatism? To what extent do magmas derive from the deep continental lithosphere? Are continental boundary layers significant trace-element reservoirs? Could they be important source rocks for certain types of ore deposits? What processes control the rise and fall of elevation for presumably stable continental interiors? What is the role of erosion in continental evolution? How does asthenosphere thickness vary beneath continents?

Finally, to what extent do continent formation and destruction influence long-term climate change? Answering these questions will inevitably require synthesis of many disparate data sets, ranging from petrology to geophysics and beyond.

## DISCLOSURE STATEMENT

The authors are not aware of any affiliations, memberships, funding, or financial holdings that might be perceived as affecting the objectivity of this review.

## ACKNOWLEDGMENTS

Discussions with N. Arndt, M. Barth, M. Bostock, G. Brimhall, Jr., R. Carlson, D. Canil, R. Dasgupta, M. Ducea, D. Eaton, G. Hirth, D. Ionov, M. Kopylova, A. Lenardic, A. Levander, S. Z.-X. Li, S.J. Mackwell, W. McDonough, F. Niu, S. Parman, G. Pearson, A. Peslier, S. Shirey, and R. Walker over the years are appreciated. We especially thank R. Rudnick, V. Le Roux, and T. Höink for discussions. This work was supported by the Packard Foundation and U.S. NSF grants to C.-T.A.L. (EAR-0309121, -0549268, -0365338, -0745540).



## LITERATURE CITED

Alard O, Griffin WL, Lorand JP, Jackson SE, O'Reilly SY. 2000. Non-chondritic distribution of the highly siderophile elements in mantle sulphides. *Nature* 407:891–94

Alard O, Griffin WL, Pearson NJ, Lorand J-P, O'Reilly SY. 2002. New insights into the Re-Os systematics of subcontinental lithospheric mantle from in situ analysis of sulphides. *Earth Planet. Sci. Lett.* 203:651–63

Arai S, Ishimaru S. 2008. Insights into petrological characteristics of the lithosphere of mantle wedge beneath arcs through peridotite xenoliths: a review. *J. Petrol.* 49:665–95

Arndt NT, Coltice N, Helmstaedt H, Gregoire M. 2009. Origin of Archean subcontinental lithospheric mantle: some petrological constraints. *Lithos* 109:61–71

Artemieva IM, Mooney WD. 2001. Thermal thickness and evolution of Precambrian lithosphere: a global study. *J. Geophys. Res.* 106:16387–414

Aubaud C, Hirschmann MM, Withers AC, Hervig RL. 2008. Hydrogen partitioning between melt, clinopyroxene, and garnet at 3 GPa in a hydrous MORB with 6 wt.% $H_2O$. *Contrib. Mineral. Petrol.* 156:607–25

Bai Q, Kohlstedt DL. 1993. Effects of chemical environment on the solubility and incorporation mechanism for hydrogen in olivine. *Phys. Chem. Miner.* 19:460–71

Barth MG, Rudnick RL, Horn I, McDonough WF, Spicuzza MJ, et al. 2001. Geochemistry of xenolithic eclogites from West Africa, part I: a link between low MgO eclogites and Archean crust formation. *Geochim. Cosmochim. Acta* 65:1499–527

Barth MG, Rudnick RL, Horn I, McDonough WF, Spicuzza MJ, et al. 2002. Geochemistry of xenolithic eclogites from West Africa, part 2: origins of the high MgO eclogites. *Geochim. Cosmochim. Acta* 66:4325–45

Beard BL, Fraracci KN, Taylor LA, Snyder GA, Clayton RN, et al. 1996. Petrography and geochemistry of eclogites from the Mir kimberlite, Yakutia, Russia. *Contrib. Mineral. Petrol.* 125:293–310

Bedini RM, Bodinier J-L, Dautria JM, Morten L. 1997. Evolution of LILE-enriched small melt fractions in the lithospheric mantle: a case study from the East African Rift. *Earth. Planet. Sci. Lett.* 153:67–83

Bennett VC, Nutman AP, McCulloch MT. 1993. Nd isotopic evidence for transient, highly depleted mantle reservoirs in the early history of the Earth. *Earth Planet. Sci. Lett.* 119:299–317

Bernstein S, Kelemen PB, Brooks CK. 1998. Depleted spinel harzburgite xenoliths in Tertiary dykes from East Greenland: restites from high degree melting. *Earth Planet. Sci. Lett.* 154:221–35

Bernstein S, Kelemen PB, Hanghoj K. 2007. Consistent olivine Mg# in cratonic mantle reflects Archean mantle melting to the exhaustion of orthopyroxene. *Geology* 35:459–62

Bostock M. 1999. Seismic imaging of lithospheric discontinuities and continental evolution. *Lithos* 48:1–16

Boyd FR. 1987. High- and low-temperature garnet peridotite xenoliths and their possible relation to the lithosphere-asthenosphere boundary beneath southern Africa. In *Mantle Xenoliths*, ed. PH Nixon, pp. 403–12. New York: Wiley

Boyd FR. 1989. Compositional distinction between oceanic and cratonic lithosphere. *Earth Planet. Sci. Lett.* 96:15–26

Boyd FR, Mertzman SA. 1987. Composition and structure of the Kaapvaal lithosphere, Southern Africa. *Geochem. Soc. Spec. Publ.* 1:13–24

Boyd FR, Pearson DG, Nixon PH, Mertzman SA. 1993. Low-calcium garnet hazburgites from southern Africa: their relations to craton structure and diamond crystallization. *Contrib. Mineral. Petrol.* 113:352–66

Boyd FR, Pokhilenko NP, Pearson DG, Mertzman SA, Sobolev NV, Finger LW. 1997. Composition of the Siberian cratonic mantle: evidence from Udachnaya peridotite xenoliths. *Contrib. Mineral. Petrol.* 128:228–46

Brey GP, Kohler T. 1990. Geothermobarometry in four-phase lherzolites II. New thermobarometers, and practical assessment of existing thermobarometers. *J. Petrol.* 31:1353–78

Cammarano F, Romanowicz B. 2007. Insights into the nature of the transition zone from physically constrained inversion of long-period seismic data. *Proc. Natl. Acad. Sci. USA* 104:9139–44

Canil D. 1991. Experimental evidence for the exsolution of cratonic peridotite from high-temperature harzburgite. *Earth Planet. Sci. Lett.* 106:64–72

Canil D. 2004. Mildly incompatible elements in peridotites and the origins of mantle lithosphere. *Lithos* 77:375–93

Canil D. 2008. Canada's craton: a bottoms-up view. *GSA Today* 18:4–10

Canil D, Lee C-TA. 2009. Were deep cratonic mantle roots hydrated in Archean oceans? *Geology* 37:667–70

Carlson RW, Irving AJ. 1994. Depletion and enrichment history of subcontinental lithospheric mantle: an Os, Sr, Nd and Pb isotopic study of ultramafic xenoliths from the northwestern Wyoming Craton. *Earth Planet. Sci. Lett.* 126:457–72

Carlson RW, Pearson DG, James DE. 2005. Physical, chemical, and chronological characteristics of continental mantle. *Rev. Geophys.* 43:RG1001

Carswell DA, Clarke DB, Mitchell RH. 1979. The petrology and geochemistry of ultramafic nodules from Pipe 200, Northern Lesotho. In *The Mantle Sample: Inclusions in Kimberlites and Other Volcanics*, ed. FR Boyd, HOA Meyer, pp. 127–44. Washington, DC: AGU

Cartigny P, Harris JW, Javoy M. 1998. Eclogitic diamond formation at Jwaneng: no room for a recycled component. *Science* 280:1421–24

Chamberlain KR, Frost CD, Frost BR. 2003. Early Archean to Mesoproterozoic evolution of the Wyoming province: Archean origins to modern lithospheric architecture. *Can. J. Earth Sci.* 40:1357–74

Chesley JT, Rudnick RL, Lee C-T. 1999. Re-Os systematics of mantle xenoliths from the East African Rift: age, structure, and history of the Tanzanian craton. *Geochim. Cosmochim. Acta* 63:1203–17

Cohen RS, O'Nions RK, Dawson JB. 1984. Isotope geochemistry of xenoliths from East Africa: implications for development of mantle reservoirs and their interaction. *Earth Planet. Sci. Lett.* 68:209–20

Condie KC. 2005. TTGs and adakites: are they both slab melts? *Lithos* 80:33–44

Condie KC, Belousova E, Griffin WL, Sircombe KN. 2009. Granitoid events in space and time: constraints from igneous and detrital zircon age spectra. *Gondwana Res.* 15:228–42

Conrad CP, Molnar P. 1997. The growth of Rayleigh-Taylor-type instabilities in the lithosphere for various rheological and density structures. *Geophys. J. Int.* 129:95–112

Cooper CM, Conrad CP. 2009. Does the mantle control the maximum thickness of cratons? *Lithosphere* 1:67–72

Cooper CM, Lenardic A, Levander A, Moresi L. 2006. Creation and preservation of cratonic lithosphere: seismic constraints and geodynamic models. *AGU Monogr.* 164:75–88

Cooper CM, Lenardic A, Moresi L. 2004. The thermal structure of stable continental lithosphere within a dynamic mantle. *Earth Planet. Sci. Lett.* 222:807–17

Cox KG, Smith MR, Beswetherick S. 1987. Textural studies of garnet lherzolites: evidence of exsolution origin from high-temperature harzburgites. In *Mantle Xenoliths*, ed. PH Nixon, pp. 537–50. New York: Wiley

Dalton CA, Ekström G, Dziewonski A. 2009. Global seismological shear velocity and attenuation: a comparison with experimental observations. *Earth Planet. Sci. Lett.* 284:65–75

Dasgupta R, Hirschmann MM, Smith ND. 2007. Water follows carbon: $CO_2$ incites deep silicate melting and dehydration beneath mid-ocean ridges. *Geology* 35:135–38
Dautria JM, Dupuy C, Takherist D, Dostal J. 1992. Carbonate metasomatism in the lithospheric mantle: peridotitic xenoliths from a melilititic district of the Sahara basin. *Contrib. Mineral. Petrol.* 111:37–52
Dawson JB. 1987. Metasomatized harzburgites in kimberlite and alkaline magmas: enriched restites and "flushed" lherzolites. In *Mantle Metasomatism*, ed. MA Menzies, CJ Hawkesworth, pp. 125–44. London: Academic
Dawson JB, Smith JV. 1977. The MARID (mica-amphibole-rutile-ilmenite-diopside) suite of xenoliths in kimberlite. *Geochim. Cosmochim. Acta* 41:309–23
DeCelles PG, Ducea MN, Kapp P, Zandt G. 2009. Cyclicity in Cordilleran orogenic systems. *Nat. Geosci.* 2:251–57
Deines P, Viljoen F, Harris JW. 2001. Implications of the carbon isotope and mineral inclusion record for the formation of diamonds in the mantle underlying a mobile belt: Venetia, South Africa. *Geochim. Cosmochim. Acta* 65:813–38
Dick HJB, Bullen T. 1984. Chromian spinel as a petrogenetic indicator in abyssal and alpine-type peridotites and spatially associated lavas. *Contrib. Mineral. Petrol.* 86:54–76
Dickinson WR, Snyder WS. 1978. Plate tectonics of the Laramide orogeny. *Mem. Geol. Soc. Am.* 151:355–66
Ducea MN, Saleeby JB. 1996. Buoyancy sources for a large, unrooted mountain range, the Sierra Nevada, California: evidence from xenolith thermobarometry. *J. Geophys. Res.* 101:8229–44
Ducea MN, Saleeby JB. 1998. The age and origin of a thick mafic-ultramafic keel from beneath the Sierra Nevada batholith. *Contrib. Mineral. Petrol.* 133:169–85
Eaton DW, Darbyshire F, Evans RL, Grutter H, Jones AG, Yuan X. 2009. The elusive lithosphere-asthenosphere boundary (LAB) beneath cratons. *Lithos* 109:1–22
Eggler DH, Meen JK, Welt F, Dudas FO, Furlong KP, et al. 1988. Tectonomagmatism of the Wyoming Province. *Colo. Sch. Mines Q.* 83:25–40
Ehrenberg SN. 1982. Petrogenesis of garnet lherzolite and megacrystalline nodules from the Thumb, Navajo volcanic field. *J. Petrol.* 23:507–47
Ellis DJ, Green EH. 1979. An experimental study of the effect of Ca upon garnet-clinopyroxene Fe-Mg exchange equilibria. *Contrib. Mineral. Petrol.* 66:13–22
Elthon D. 1992. Chemical trends in abyssal peridotites: refertilization of depleted suboceanic mantle. *J. Geophys. Res.* 97:9015–25
Farquhar J, Wing BA, McKeegan KD, Harris JW, Cartigny P, Thiemens MH. 2002. Mass-independent sulfur of inclusions in diamond and sulfur recycling on early Earth. *Science* 2002:2369–72
Fischer KM, Ford HA, Abt DL, Rychert CA. 2010. The lithosphere-asthenosphere boundary. *Annu. Rev. Earth Planet. Sci.* 38:551–75
Foley SF. 2008. Rejuvenation and erosion of the cratonic lithosphere. *Nat. Geosci.* 1:503–10
Foley SF, Tiepolo M, Vannucci R. 2002. Growth of early continental crust controlled by melting of amphibolite in subduction zones. *Nature* 417:837–40
Fung AT, Haggerty SE. 1995. Petrography and mineral composition of eclogites from the Koidu Kimberlite Complex, Sierra Leone. *J. Geophys. Res.* 100:20451–73
Gao S, Rudnick RL, Carlson RW, McDonough WF, Liu Y. 2002. Re-Os evidence for replacement of ancient mantle lithosphere beneath the North China Craton. *Earth Planet. Sci. Lett.* 198:307–22
Goes S, van der Lee S. 2002. Thermal structure of the North American uppermost mantle inferred from seismic tomography. *J. Geophys. Res.* 107(B3):2050
Goodwin AM. 1991. *Principles of Precambrian Geology*. London: Academic. 666 pp.
Grant K, Ingrin J, Lorand JP, Dumas P. 2007. Water partitioning between mantle minerals from peridotite xenoliths. *Contrib. Mineral. Petrol.* 154:15–34
Gregory RT, Taylor HP Jr. 1981. An oxygen isotope profile in a section of Cretaceous oceanic crust, Samail Ophiolite, Oman: evidence for $\delta^{18}O$ buffering of the oceans by deep (>5 km) seawater-hydrothermal circulation at mid-ocean ridges. *J. Geophys. Res.* 86(B4):2737–55
Griffin WL, O'Reilly SY. 2007. Cratonic lithospheric mantle: is anything subducted? *Episodes* 30:43–53
Griffin WL, O'Reilly SY, Abe N, Aulbach S, Davies RM, et al. 2003. The origin and evolution of Archean lithospheric mantle. *Precambrian Res.* 127:19–41

Griffin WL, O'Reilly SY, Ryan CG. 1999. The composition and origin of subcontinental lithospheric mantle. *Geochem. Soc. Spec. Publ.* 6:13–45

Griffin WL, Zhang AD, O'Reilly SY, Ryan CG. 1998. Phanerozoic evolution of the lithosphere beneath the Sino-Korean craton. In *Mantle Dynamics and Plate Interactions in East Asia*, ed. MFJ Flower, S-L Chung, C-H Lo, T-Y Lee, pp. 107–26. Washington, DC: AGU

Gung Y, Panning M, Romanowicz B. 2003. Global anisotropy and the thickness of continents. *Nature* 422:707–11

Handler MR, Bennet VC, Esat TM. 1997. The persistence of off-cratonic lithospheric mantle: Os isotopic systematics of variably metasomatized southeast Australian xenoliths. *Earth Planet. Sci. Lett.* 151:61–75

Hansen S, Dueker K. 2009. P- and S-wave receiver function images of crustal imbrication beneath the Cheyenne Belt in southeast Wyoming. *Bull. Seismol. Soc. Am.* 99:1953–61

Hanson GN, Langmuir C. 1978. Modeling of major elements in mantle-melt systems using trace element approaches. *Geochim. Cosmochim. Acta* 42:725–41

Harley SL, Green DH. 1982. Garnet-orthopyroxene barometry for granulites and peridotites. *Nature* 300:697–701

Hawkesworth C, Kemp AIS. 2006. Evolution of the continental crust. *Nature* 443:811–17

Helmstaedt H, Schulze DJ. 1989. Southern African kimberlites and their mantle sample: implication for Archean tectonics and lithosphere evolution. *Geol. Soc. Aust. Spec. Publ.* 14:358–68

Herzberg C. 2004. Geodynamic information in peridotite petrology. *J. Petrol.* 45:2507–30

Herzberg C, Condie KC, Korenaga J. 2010. Thermal history of the Earth and its petrological expression. *Earth Planet. Sci. Lett.* 292:79–88

Herzberg CT. 1993. Lithosphere peridotites of the Kaapvaal craton. *Earth Planet. Sci. Lett.* 120:13–29

Hirschmann MM. 2006. Water, melting, and the deep Earth $H_2O$ cycle. *Annu. Rev. Earth Planet. Sci.* 34:629–53

Hirth G, Evans RL, Chave AD. 2000. Comparison of continental and oceanic mantle electrical conductivity: Is the Archean lithosphere dry? *Geochem. Geophys. Geosys.* 1(12):1030

Hirth G, Kohlstedt DL. 1996. Water in the oceanic upper mantle: implications for rheology, melt extraction and the evolution of the lithosphere. *Earth Planet. Sci. Lett.* 144:93–108

Hoffman PF. 1989. Precambrian geology and tectonic history of North America. In *The Geology of North America—an Overview*, ed. AW Bally, AR Palmer, pp. 447–511. Boulder, CO: Geol. Soc. Am.

Hofmann AW. 1997. Mantle geochemistry: the message from oceanic volcanism. *Nature* 385:219–29

Horodyskyj U, Lee C-TA, Ducea MN. 2007. Similarities between Archean high MgO eclogites and Phanerozoic arc-eclogite cumulates and the role of arcs in Archean continent formation. *Earth Planet. Sci. Lett.* 256:510–20

Houseman GA, Molnar PA. 1997. Gravitational (Rayleigh-Taylor) instability of a layer with nonlinear viscosity and convective thinning of continental lithosphere. *Geophys. J. Int.* 128:125–50

Huang J, Zhong S, van Hunen J. 2003. Controls on sublithospheric small-scale convection. *J. Geophys. Res.* 108(B8):2405

Humphreys ED, Hessler E, Dueker KG, Farmer GL, Erslev EA, Atwater TA. 2003. How Laramide-age hydration of North American lithosphere by the Farallon slab controlled subsequent activity in the western United States. *Int. Geol. Rev.* 45:575–95

Ionov DA, Bodinier J-L, Mukasa SB, Zanetti A. 2002. Mechanisms and sources of mantle metasomatism: major and trace element compositions of peridotite xenoliths from Spitsbergen in the context of numerical modeling. *J. Petrol.* 43:2219–59

Ionov DA, Chanefo I, Bodinier J-L. 2005. Origin of Fe-rich lherzolites and wehrlites from Tok, SE Siberia by reactive melt percolation in refractory mantle peridotites. *Contrib. Mineral. Petrol.* 150:335–53

Ionov DA, Dupuy C, O'Reilly SY, Kopylova MG, Genshaft YS. 1993. Carbonated peridotite xenoliths from Spitsbergen: implications for trace element signature of mantle carbonate metasomatism. *Earth Planet. Sci. Lett.* 119:283–97

Jacob DE. 2004. Nature and origin of eclogite xenoliths in kimberlites. *Lithos* 77:295–316

Jagoutz OE, Burg J-P, Hussain S, Dawood H, Pettke T, et al. 2009. Construction of the granitoid crust of an island arc part I: geochronological and geochemical constraints from the plutonic Kohistan (NW Pakistan). *Contrib. Mineral. Petrol.* 158:739–55

Jordan TH. 1978. Composition and development of the continental tectosphere. *Nature* 274:544–48
Jordan TH. 1979. Mineralogies, densities and seismic velocities of garnet lherzolites and their geophysical implications. In *The Mantle Sample: Inclusions in Kimberlites and Other Volcanics*, ed. FR Boyd, HOA Meyer, pp. 1–14. Washington, DC: AGU
Jordan TH. 1988. Structure and formation of the continental tectosphere. *J. Petrol.* 1988:11–37
Katz RF, Spiegelman M, Langmuir CH. 2003. A new parameterization of hydrous mantle melting. *Geochem. Geophys. Geosys.* 4(9):1073
Kay SM, Godoy E, Kurtz A. 2005. Episodic arc migration, crustal thickening, subduction erosion and magmatism in the south-central Andes. *Geol. Soc. Am. Bull.* 117:67–88
Kelemen PB, Hart SR, Bernstein S. 1998. Silica enrichment in the continental upper mantle via melt/rock reaction. *Earth. Planet. Sci. Lett.* 164:387–406
Kelemen PB, Shimizu N, Dunn T. 1993. Relative depletion of niobium in some arc magmas and the continental crust: partitioning of K, Nb, La and Ce during melt/rock reaction in the upper mantle. *Earth Planet. Sci. Lett.* 120:111–34
Kelly RK, Kelemen PB, Jull M. 2003. Buoyancy of the continental upper mantle. *Geochem. Geophys. Geosys.* 4:1017
King SD. 2005. Archean cratons and mantle dynamics. *Earth Planet. Sci. Lett.* 234:1–14
Kohlstedt DL, Mackwell SJ. 1998. Diffusion of hydrogen and intrinsic point defects in olivine. *Ztg. Phys. Chem.* 207:147–62 (In German)
Kopylova MG, Russell JK. 2000. Chemical stratification of cratonic lithosphere: constraints from the northern Slave Craton, Canada. *Earth Planet. Sci. Lett.* 181:71–87
Kopylova MG, Russell JK, Cookenboo H. 1999. Petrology of peridotite and pyroxenite xenoliths from Jericho Kimberlite: implications for the thermal state of the mantle beneath the Slave Craton, northern Canada. *J. Petrol.* 40:79–104
Korenaga J, Jordan TH. 2003. Physics of multiscale convection in Earth's mantle: onset of sublithospheric convection. *J. Geophys. Res.* 108(B7):2333
Le Roux V, Bodinier J-L, Tommasi A, Alard O, Dautria JM, et al. 2007. The Lherz spinel lherzolite: refertilized rather than pristine mantle. *Earth Planet. Sci. Lett.* 259:599–612
Lee C-T, Rudnick RL. 1999. Compositionally stratified cratonic lithosphere: petrology and geochemistry of peridotite xenoliths from the Labait Volcano, Tanzania. In *Proc. 7th Int. Kimberl. Conf., J.B. Dawson Vol.*, ed. JJ Gurney, JL Gurney, MD Pascoe, SR Richardson, pp. 503–21. Cape Town, S. Afr.: Univ. Cape Town
Lee C-T, Yin Q, Rudnick RL, Jacobsen SB. 2001. Preservation of ancient and fertile lithospheric mantle beneath the southwestern United States. *Nature* 411:69–73
Lee C-TA. 2003. Compositional variation of density and seismic velocities in natural peridotites at STP conditions: implications for seismic imaging of compositional heterogeneities in the upper mantle. *J. Geophys. Res.* 108:2441
Lee C-TA. 2005. Trace element evidence for hydrous metasomatism at the base of the North American lithosphere and possible association with Laramide low-angle subduction. *J. Geol.* 113:673–85
Lee C-TA. 2006. Geochemical/petrologic constraints on the origin of cratonic mantle. In *Archean Geodynamics and Environments*, ed. K Benn, J-C Mareschal, KC Condie, *Geophys. Monogr.* 164:89–114. Washington, DC: AGU
Lee C-TA, Cheng X, Horodyskyj U. 2006. The development and refinement of continental arcs by primary basaltic magmatism, garnet pyroxenite accumulation, basaltic recharge and delamination: insights from the Sierra Nevada, California. *Contrib. Mineral. Petrol.* 151:222–42
Lee C-TA, Lenardic A, Cooper CM, Niu F, Levander A. 2005. The role of chemical boundary layers in regulating the thickness of continental and oceanic thermal boundary layers. *Earth Planet. Sci. Lett.* 230:379–95
Lee C-TA, Luffi P, Höink T, Li Z-XA, Lenardic A. 2008. The role of serpentine in preferential craton formation in the late Archean by lithosphere underthrusting. *Earth Planet. Sci. Lett.* 269:96–104
Lee C-TA, Luffi P, Plank T, Dalton HA, Leeman WP. 2009. Constraints on the depths and temperatures of basaltic magma generation on Earth and other terrestrial planets using new thermobarometers for mafic magmas. *Earth Planet. Sci. Lett.* 279:20–33

Lenardic A, Moresi L-N, Muhlhaus H-B. 2003. Longevity and stability of cratonic lithosphere: insights from numerical simulations of coupled mantle convection and continental tectonics. *J. Geophys. Res.* 108(B6):2303

Levander A, Niu F, Lee C-TA, Cheng X. 2005. Imag(in)ing the continental lithosphere. *Tectonophysics* 416: 167–85

Li Z-XA, Lee C-TA, Peslier AH, Lenardic A, Mackwell SJ. 2008. Water contents in mantle xenoliths from the Colorado Plateau and vicinity: implications for the rheology and hydration-induced thinning of continental lithosphere. *J. Geophys. Res.* 113:B09210

Luffi P, Saleeby J, Lee C-TA, Ducea MN. 2009. Lithospheric mantle duplex beneath the central Mojave Desert revealed by xenoliths from Dish Hill, California. *J. Geophys. Res.* 114:B03202

Mackwell SJ, Kohlstedt DL. 1990. Diffusion of hydrogen in olivine: implications for water in the mantle. *J. Geophys. Res.* 95:5079–88

Mattey D, Lowry D, Macpherson C. 1994. Oxygen isotope composition of mantle peridotite. *Earth Planet. Sci. Lett.* 128:231–41

McDonough WF, Sun S-S. 1995. The composition of the Earth. *Chem. Geol.* 120:223–53

Mei S, Kohlstedt DL. 2000a. Influence of water on plastic deformation of olivine aggregates 1. Diffusion creep regime. *J. Geophys. Res.* 105:21457–69

Mei S, Kohlstedt DL. 2000b. Influence of water on plastic deformation of olivine aggregates 2. Dislocation creep regime. *J. Geophys. Res.* 105:21471–81

Menzies M, Fan W-M, Zhang M. 1993. Paleozoic and Cenozoic lithoprobes and the loss of >120 km of Archean lithosphere, Sino-Korean craton, China. *Geol. Soc. Lond. Spec. Publ.* 76:71–81

Menzies M, Xu Y, Zhang H, Fan W. 2007. Integration of geology, geophysics and geochemistry: a key to understanding the North China craton. *Lithos* 96:1–21

Molnar P, Houseman GA, Conrad CP. 1998. Rayleigh-Taylor instability and convective thinning of mechanically thickened lithosphere: effects of nonlinear viscosity decreasing exponentially with depth and of horizontal shortening of the layer. *Geophys. J. Int.* 133:568–84

Nettles M, Dziewonski A. 2008. Radially anisotropic shear velocity structure of the upper mantle globally and beneath North America. *J. Geophys. Res.* 113:B02303

Niu F, Levander A, Cooper CM, Lee C-TA, Lenardic A, James DE. 2004. Seismic constraints on the depth and composition of the mantle keel beneath the Kaapvaal craton. *Earth Planet. Sci. Lett.* 224:337–46

Nixon PH, Rogers NW, Gibson IL, Grey A. 1981. Depleted and fertile mantle xenoliths from southern African kimberlites. *Annu. Rev. Earth Planet. Sci.* 9:285–309

Nyblade A. 1999. Heat flow and the structure of the Precambrian lithosphere. *Lithos* 48:81–91

O'Neill HSC. 1981. The transition between spinel lherzolite and garnet lherzolite, and its use as a geobarometer. *Contrib. Mineral. Petrol.* 77:185–94

Parman SW, Grove TL, Dann JC, de Wit MJ. 2004. A subduction origin for komatiites and cratonic lithospheric mantle. *S. Afr. J. Geol.* 107:107–18

Pearson DG, Canil D, Shirey S. 2003. Mantle samples included in volcanic rocks: xenoliths and diamonds. In *Treatise of Geochemistry*, ed. HD Holland, KK Turekian, pp. 171–275. Oxford: Elsevier

Pearson DG, Carlson RW, Shirey SB, Boyd FR, Nixon PH. 1995a. Stabilization of Archean lithospheric mantle: a Re-Os isotope study of peridotite xenoliths from the Kaapvaal craton. *Earth Planet. Sci. Lett.* 134:341–57

Pearson DG, Nowell GM. 2002. The continental lithospheric mantle: characteristics and significance as a mantle reservoir. *Philos. Trans. R. Soc. Lond. Ser. A* 360:2383–410

Pearson DG, Shirey SB, Carlson RW, Boyd FR, Pokhilenko NP, Shimizu N. 1995b. Re-Os, Sm-Nd, and Rb-Sr isotope evidence for thick Archean lithospheric mantle beneath the Siberian craton modified by multistage metasomatism. *Geochim. Cosmochim. Acta* 59:959–77

Pearson DG, Wittig N. 2008. Formation of Archean continental lithosphere and its diamonds: the root of the problem. *J. Geol. Soc.* 165:895–914

Pedersen HA, Fishwick S, Snyder DB. 2009. A comparison of cratonic roots through consistent analysis of seismic surface waves. *Lithos* 109:81–95

Peslier AH. 2010. A review of water contents of nominally anhydrous natural minerals in the mantles of Earth, Mars and the Moon. *J. Volcanol. Geotherm. Res.* 197:239–58

Peslier AH, Snow JE, Hellebrand E, Von Der Handt A. 2007. *Low water contents in minerals from the Gakkel ridge abyssal peridotites, Arctic Ocean*. Presented at Goldschmidt Conf., Cologne, Ger.
Pollack HN. 1986. Cratonization and thermal evolution of the mantle. *Earth Planet. Sci. Lett.* 80:175–82
Pollack HN, Hurter SJ, Johnson JR. 1993. Heat flow from the Earth's interior: analysis of the global data set. *Rev. Geophys.* 31:267–80
Pyle JM, Haggerty SE. 1998. Eclogites and the metasomatism of eclogites from the Jagersfontein Kimberlite: punctuated transport and implications for alkali magmatism. *Geochim. Cosmochim. Acta* 62:1207–31
Rapp RP, Shimizu N, Norman MD. 2003. Growth of early continental crust by partial melting of eclogite. *Nature* 425:605–9
Reisberg L, Lorand J-P. 1995. Longevity of subcontinental mantle lithosphere from osmium isotope systematics in orogenic peridotite massifs. *Nature* 376:159–62
Richardson SH, Gurney JJ, Erlank AJ, Harris JW. 1984. Origin of diamonds in old enriched mantle. *Nature* 310:198–202
Roden MF, Murthy VR. 1985. Mantle metasomatism. *Annu. Rev. Earth Planet. Sci.* 13:269–96
Rollinson HR. 1997. Eclogite xenoliths in West African kimberlites as residues from Archean granitoid crust formation. *Nature* 389:173–76
Rowe MC, Lassiter JC. 2009. Chlorine enrichment in central Rio Grande Rift basaltic melt inclusions: evidence for subduction modification of the lithospheric mantle. *Geology* 37:439–42
Rudnick RL, Gao S, Ling W-L, Liu Y-S, McDonough WF. 2004. Petrology and geochemistry of spinel peridotite xenoliths from Hannuoba and Qixia, North China craton. *Lithos* 77:609–37
Rudnick RL, Ireland TR, Gehrels G, Irving AJ, Chesley JT, Hanchar JM. 1999. *Dating mantle metasomatism: U-Pb geochronology of zircons in cratonic mantle xenoliths from Montana and Tanzania*. Presented at 7th Int. Kimberl. Conf., Rondebosch, S. Afr.
Rudnick RL, McDonough WF, Chappell BW. 1993. Carbonatite metasomatism in the northern Tanzanian mantle: petrographic and geochemical characteristics. *Earth Planet. Sci. Lett.* 114:463–75
Rudnick RL, McDonough WF, O'Connell RJ. 1998. Thermal structure, thickness and composition of continental lithosphere. *Chem. Geol.* 145:395–411
Rudnick RL, McDonough WF, Orpin A. 1994. Northern Tanzanian peridotite xenoliths: a comparison with Kaapvaal peridotites and inferences of metasomatic reactions. *Proc. 5th Int. Kimberl. Conf., Araxa, Braz.*, pp. 336–53. Brasilia, Braz.: CPRM
Rychert CA, Shearer PM. 2009. A global view of the lithosphere-asthenosphere boundary. *Science* 324:495–98
Saleeby J. 2003. Segmentation of the Laramide Slab—evidence from the southern Sierra Nevada region. *Geol. Soc. Am. Bull.* 115:655–68
Saleeby J, Ducea M, Clemens-Knott D. 2003. Production and loss of high-density batholithic root, southern Sierra Nevada, California. *Tectonics* 22(6):1064
Saltzer RL, Chatterjee N, Grove TL. 2001. The spatial distribution of garnets and pyroxenes in mantle peridotites: pressure-temperature history of peridotites from the Kaapvaal craton. *J. Petrol.* 42:2215–29
Schulze DJ. 1989. Constraints on the abundance of eclogite in the upper mantle. *J. Geophys. Res.* 94:4205–12
Schutt DL, Lesher CE. 2006. Effects of melt depletion on the density and seismic velocity of garnet and spinel lherzolite. *J. Geophys. Res.* 111:B05401
Seber D, Barazangi M, Ibenbrahim A, Demnati A. 1996. Geophysical evidence for lithospheric delamination beneath the Alboran Sea and Rif-Betic Mountains. *Nature* 379:785–90
Şengör AMC, Natal'in BA, Burtman VS. 1993. Evolution of the Altaid tectonic collage and Paleozoic crustal growth in Eurasia. *Nature* 364:299–307
Shirey SB, Harris JW, Richardson SR, Fouch MJ, James DE, et al. 2002. Diamond genesis, seismic structure, and evolution of the Kaapvaal-Zimbabwe craton. *Science* 297:1683–86
Shirey SB, Walker RJ. 1998. The Re-Os isotope system in cosmochemistry and high-temperature geochemistry. *Annu. Rev. Earth Planet. Sci.* 26:423–500
Simon NSC, Carlson RW, Pearson DG, Davies GR. 2007. The origin and evolution of the Kaapvaal cratonic lithospheric mantle. *J. Petrol.* 48:589–625
Sleep NH. 2004. Evolution of the continental lithosphere. *Annu. Rev. Earth Planet. Sci.* 33:369–93
Smith D. 2000. Insights into the evolution of the uppermost continental mantle from xenolith localities on and near the Colorado Plateau and regional comparisons. *J. Geophys. Res.* 2000:16769–81

Smith D. 2010. Antigorite peridotite, metaserpentinite, and other inclusions within diatremes on the Colorado Plateau, SW USA: implications for the mantle wedge during low-angle subduction. *J. Petrol.* 51:1355–79

Smith D, Riter JC, Mertzman SA. 1999. Water-rock interactions, orthopyroxene growth, and Si-enrichment in the mantle: evidence in xenoliths from the Colorado Plateau, southwestern United States. *Earth Planet. Sci. Lett.* 165:45–54

Smithies RH. 2000. The Archean tonalite-trondhjemite-granodiorite (TTG) series is not an analogue of Cenozoic adakite. *Earth Planet. Sci. Lett.* 182:115–25

Song S, Yang J, Liou JG, Wu C, Shi R, Xu Z. 2003. Petrology, geochemistry and isotopic ages of eclogites from the Dulan UHPM Terrane, the North Qaidam, NW China. *Lithos* 70:195–211

Taylor LA, Neal CR. 1989. Eclogites with oceanic crustal and mantle signatures from the Bellsbank kimberlite, South Africa, Part I: mineralogy, petrography, and whole rock chemistry. *J. Geol.* 97:551–67

Taylor LA, Snyder GA, Keller R, Remley DA, Anand M, et al. 2003. Petrogenesis of group A eclogites and websterites: evidence from the Obnazhennaya kimberlite, Yakutia. *Contrib. Mineral. Petrol.* 145:424–43

Tenner T, Hirschmann MM, Withers AC, Hervig RL. 2009. Hydrogen partitioning between nominally anhydrous upper mantle minerals and melt between 3 and 5 GPa and applications to hydrous peridotite partial melting. *Chem. Geol.* 262:42–56

Walker RJ, Carlson RW, Shirey SB, Boyd FR. 1989. Os, Sr, Nd, and Pb isotope systematics of southern African peridotite xenoliths: implications for the chemical evolution of subcontinental mantle. *Geochim. Cosmochim. Acta* 53:1583–95

Walter MJ. 1999. Melting residues of fertile peridotite and the origin of cratonic lithosphere. *Geochem. Soc. Spec. Publ.* 6:225–39

Walter MJ. 2003. Melt extraction and compositional variability in mantle lithosphere. In *The Mantle and Core: Treatise on Geochemistry, Vol. 2*, ed. RW Carlson, pp. 363–94. Oxford: Elsevier-Pergamon

Winterburn PA, Harte B, Gurney JJ. 1989. Peridotite xenoliths from the Jagersfontein kimberlite pipe: I. Primary and primary-metasomatic mineralogy. *Geochim. Cosmochim. Acta* 54:329–41

Wittig N, Pearson DG, Webb M. 2008. Origin of cratonic lithosphere mantle roots: a geochemical study of peridotites from the North Atlantic Craton, West Greenland. *Earth Planet. Sci. Lett.* 274:24–33

Yang X-Z, Xia Q-K, Deloule E, Dallai L, Fan QC, Feng M. 2008. Water in minerals of the continental lithospheric mantle and overlying lower crust: a comparative study of peridotite and granulite xenoliths from the North China craton. *Chem. Geol.* 256:33–45

Yaxley GM, Crawford AJ, Green DH. 1991. Evidence for carbonatite metasomatism in spinel peridotite xenoliths from western Victoria, Australia. *Earth Planet. Sci. Lett.* 107:305–17

Zindler A, Jagoutz E. 1988. Mantle cryptology. *Geochim. Cosmochim. Acta* 52:319–33

Annual Review
of Earth and
Planetary Sciences
Volume 39, 2011

# Contents

**Indexes**



**Errata**

An online log of corrections to *Annual Review of Earth and Planetary Sciences* articles may be found at http://earth.annualreviews.org